



Review article

Bio-inspired control strategies in wearable robotics: A comprehensive review of CPGs and DMPs

Joana F. Almeida ^a*, Cristina P. Santos ^{a,b}¹^a Center for MicroElectroMechanical Systems (CMEMS), University of Minho, Guimarães, 4800-058, Portugal^b Associate Laboratory (LABBELS), University of Minho, Braga/Guimarães, 4710-057/4800-058, Portugal

ARTICLE INFO

ABSTRACT

Keywords:

Central pattern generators
 Dynamic movement primitives
 Exoskeletons
 Orthoses
 Assisted locomotion

Wearable robotic devices such as exoskeletons and orthoses have undergone significant advancements over the past two decades, aiming to support human mobility in rehabilitation, daily life, and industrial settings. Central to their effectiveness is the implementation of control strategies that generate smooth, adaptive, and user-synchronized movements. Among these, bio-inspired approaches that emulate neural and motor mechanisms of human locomotion have gained increasing attention.

This review presents a comprehensive analysis of two prominent bio-inspired control frameworks – Central Pattern Generators (CPGs) and Dynamic Movement Primitives (DMPs) – implemented in wearable lower-limb robotic systems. A total of 45 articles were systematically analysed to identify trends and challenges in their application.

The review examines the purposes of these controllers, the joints and degrees of freedom addressed, the sensors employed, the structural characteristics of each approach, the integration of sensory feedback and intention decoding, the tracking controllers used, and the validation methodologies adopted.

The findings reveal that CPGs and DMPs are primarily adopted for generating adaptive joint trajectories, enabling stable, rhythmic, and responsive locomotion. Their flexibility allows for encoding motion patterns that adapt to user-specific and task-specific requirements. However, challenges such as parameter tuning, integration of sensory feedback, real-time intention decoding, and validation robustness remain open issues.

This work highlights the potential of CPG- and DMP-based strategies to enhance the autonomy, safety, and personalization of wearable robots and provides future research directions to address their current limitations and improve their practical applicability.

Contents

1. Introduction	2
2. Conceptual overview of CPGs and DMPs.....	2
2.1. CPGs	2
2.2. DMPs	3
2.3. Conclusion	3
3. Literature search methodology	3
4. Results.....	4
4.1. Citation metrics analysis	4
4.2. Purpose	4
4.3. Devices and DoFs	5
4.4. Sensors	6
4.5. Central pattern generators	7
4.6. Dynamic movement primitives	11
4.7. Decoding motion intention	13
4.8. Tracking controllers.....	14

* Corresponding author.

E-mail addresses: pg50435@alunos.uminho.pt (J.F. Almeida), cristina@dei.uminho.pt (C.P. Santos).¹ Contributing author.

4.9. Validation procedures	14
5. Discussion	15
5.1. Applications	15
5.2. Joints controlled	15
5.3. Sensors	15
5.4. CPG structure	16
5.5. DMP structure	16
5.6. Feedback pathways	16
5.7. Detection of human intention	16
5.8. Low-level tracking controllers	17
5.9. Validation protocols	17
5.10. Outcomes	17
5.11. Challenges and limitations	18
6. Conclusion	18
Declaration of competing interest	18
Appendix A. Mathematical formulations	18
A.1. CPGs equations	18
A.2. Periodic DMPs	22
Appendix B. Summary of results and conclusions per article	22
Data availability	22
References	22

1. Introduction

As life expectancy increases, so does the demand for technologies that support, protect, rehabilitate, or enhance physical abilities (Qiu, Pei, Wang, & Tang, 2023). Wearable devices such as exoskeletons and orthoses have gained increasing attention as promising solutions in this context. These devices operate alongside the human body and are commonly used in movement assistance, rehabilitation, and human augmentation (Huang, Cheng, Guo, Lin, & Zhang, 2018; Qiu, Guo, Zha, Deng, & Wang, 2021; Young & Ferris, 2016).

Their development lies at the intersection of robotics, biomechanics, and control engineering (Sun, Tang, Zheng, Dong, Chen, & Bai, 2022). Most research adopts a hierarchical control model – first proposed by Tucker et al. (2015) and later refined by Baud, Manzoori, Ijspeert, and Bouri (2021) – comprising three layers: a high-level perception layer (for decoding intentions and needs), a mid-level layer (for generating reference trajectories), and a low-level control layer (for ensuring tracking).

Given the need for anthropomorphic and adaptive movement, traditional control strategies often fall short in meeting the complexity and variability of human locomotion (Akkawutvanich & Manoonpong, 2023; Qiu et al., 2021). This has led to increasing interest in bio-inspired models that replicate principles of natural motor control to enable more seamless and intuitive Human–Robot Interaction (HRI). These approaches aim to produce control that is more natural, robust, and adaptable to human variability. Among these strategies, Central Pattern Generators (CPGs) and Dynamic Movement Primitives (DMPs) have received particular attention. Both models rely on non-linear control formulations to generate compact movement representations and produce robust, flexible motor outputs in biological and robotic systems (Akkawutvanich & Manoonpong, 2023; Saveriano, Abu-Dakka, Kramberger, & Peternel, 2023; Yu, Tan, Chen, & Zhang, 2013).

Rather than comparing CPGs and DMPs to other control approaches, this review focuses exclusively on how these two strategies have been implemented in wearable robotics. We systematically identify and analyse studies using these methods, examining the devices and joints involved, sensor types, actuators, feedback mechanisms for real-time adaptation, and their integration in hierarchical control structures. This includes user intent decoding strategies and low-level controllers, which are critical for functional performance. We also summarize validation protocols and performance metrics employed in the literature.

This article presents the following key contributions: (i) a structured analysis of how CPGs and DMPs are implemented in wearable robotics,

considering their specific functions, sensor usage, and feedback integration; and (ii) an identification of common trends, technical challenges, and research gaps that must be addressed to advance the field. Through this, the review offers a comprehensive understanding of the current landscape of bio-inspired control in wearable robotics and outlines the remaining challenges to improve their practical implementation.

This review is organized as follows. Section 2 provides a theoretical overview of CPGs and DMPs, outlining their fundamental principles. Section 3 describes the literature search methodology adopted in this study. Section 4 presents the results, summarizing key findings across the identified topics of interest. Section 5 discusses the main insights and limitations of the current research. Finally, Section 6 concludes the article and suggests directions for future research.

2. Conceptual overview of CPGs and DMPs

Biological systems have long inspired engineers and scientists, offering innovative solutions to complex challenges through the emulation of nature's designs. They are valued for their efficiency, adaptability, and robustness when dealing with complex scenarios. As a result, applying biological principles has led to significant technological progress.

One compelling area of biological inspiration in robotics is locomotion—an inherently complex motor task that requires precise coordination of multiple joints and continuous adaptation to changing environments. Due to the remarkable ability of biological systems to perform such tasks effortlessly, bio-inspired control strategies have been developed to enhance human–robot coordination (Wu, Liu, Zhang, & Chen, 2009). Two prominent approaches within this domain are Central Pattern Generators (CPGs) and Dynamic Movement Primitives (DMPs).

2.1. CPGs

In neuroscience, CPGs are neural networks in the Central Nervous System (CNS) responsible for autonomously generating rhythmic motion patterns (Ijspeert, 2008; Yu et al., 2013). Animal studies (e.g. salamanders and cats) have shown that the CNS follows a top-down hierarchical structure, with CPGs located at the lowest level. This allows CPGs to generate complex patterns without higher-level commands or feedback—although both are necessary for movement refinement and adaptation.

In engineering, CPGs are modelled as non-linear dynamical systems capable of producing stable oscillatory outputs without requiring

external inputs (Ijspeert, 2008). This behaviour is typically modelled through differential equations with limit cycle properties, and several mathematical formulations have been proposed to represent artificial CPGs (Akkawutvanich & Manoonpong, 2023; Ijspeert, 2008; Righetti & Ijspeert, 2006; Santos, Alves, & Moreno, 2017; Yu et al., 2013).

According to Yu et al. (2013), CPG-inspired control models can be classified into four categories: neuron models, non-linear oscillator models, network models, and hybrid models. Neuron models include Hodgkin–Huxley, Stein’s model, leaky-integrator models, and others that capture fundamental neuronal behaviours (Wu et al., 2009). One of the most well-known neural oscillators was proposed by Matsuoka (1985). Non-linear oscillator models include phase oscillators (e.g., Kuramoto (Acebrón, Bonilla, Vicente, Ritort, & Spigler, 2005)), harmonic oscillators (e.g., Hopf (Wu et al., 2009)), and relaxation oscillators such as Van der Pol’s and Rayleigh’s models (Yu et al., 2013). Network models typically use a two-layer structure: one for rhythm generation and one for pattern formation. Hybrid models combine different approaches to leverage their respective advantages and improve dynamic performance.

Due to their intrinsic properties, these models produce stable and robust oscillations, even in the presence of small external disturbances. Feedback can be integrated through coupling terms that allow real-time modulation based on sensory inputs—a mechanism known as mutual entrainment (Akkawutvanich & Manoonpong, 2023; Ijspeert, 2008; Santos et al., 2017; Yu et al., 2013).

One of the key advantages of CPGs is their modular and distributed architecture. Individual CPG units are often associated with one Degree of Freedom (DoF) and can be interconnected to coordinate motion. The models typically require only a small number of parameters, each linked to a specific system property. Such design enables easy modulation of output features like amplitude, frequency, and phase—facilitating smooth transitions and increasing flexibility (Ijspeert, 2008; Yu et al., 2013). CPGs can generate trajectories in kinematic terms (position, velocity, acceleration) or dynamic terms (force or torque) for direct motor control.

CPGs also serve as a strong foundation for learning and optimization algorithms (Ijspeert, 2008; Wu et al., 2009; Yingxu, Aibin, Hongling, Pengcheng, Zhang, & Guangzhong, 2019; Yu et al., 2013). For example, in Learning from Demonstration (LfD), Adaptive Frequency Oscillators (AFOs) are used to extract rhythmic patterns, and Hebbian learning allows these systems to capture signal characteristics through a simple feedback loop (Ijspeert, 2008; Righetti & Ijspeert, 2006; Santos et al., 2017).

Together, these features highlight the value of CPGs for controlling locomotion in robotic systems, particularly in wearable devices designed for close human interaction.

2.2. DMPs

DMPs represent an alternative framework for modelling and replicating motor control in biological systems. They are based on the idea that complex movements arise from the sequencing and combination of elementary motion units—known as motion primitives (Saveriano et al., 2023). This modularity allows biological systems to adapt to dynamic environments and perform sophisticated tasks efficiently.

DMPs are mathematically modelled as non-linear dynamical systems composed of a canonical (temporal) and a transformation (spatial) component (Matos & Santos, 2014; Saveriano et al., 2023). They generate goal-directed trajectories modulated by a learnable non-linear forcing term, enabling flexible adaptation to different tasks. Two main formulations exist: point attractors, for discrete movements, and cycle attractors, for rhythmic behaviours (Saveriano et al., 2023).

The original formulation of DMPs was introduced by Ijspeert et al. in the early 2000s (Ijspeert, Nakanishi, & Schaal, 2002a, 2002b; Schaal, 2006). Since then, various adaptations have been proposed to tailor the model to different control scenarios (Saveriano et al., 2023).

DMPs share several properties with CPGs. They allow easy modulation of amplitude, frequency, and phase through explicit parameters. They also support distributed control of multi-DoF systems by combining a shared canonical system with individual transformation systems for each DoF (Saveriano et al., 2023). DMPs can output kinematic trajectories as well as torque or force profiles (Matos & Santos, 2014; Schaal, 2006).

Additionally, they support real-time adaptation via feedback coupling, making them suitable for executing dynamic, responsive movements (Matos & Santos, 2014; Qiu, Guo, Caldwell, & Chen, 2020; Saveriano et al., 2023).

DMPs are commonly implemented in LfD frameworks, enabling them to encode new motor tasks from observed demonstrations. In most cases, supervised learning is used to adjust the weights of the non-linear forcing term, allowing accurate reproduction of target trajectories (Matos & Santos, 2014; Qiu et al., 2020; Saveriano et al., 2023; Schaal, 2006).

2.3. Conclusion

Notably, some studies have combined CPGs and DMPs, leveraging their complementary characteristics. Ijspeert (Ijspeert, 2008) even proposed viewing CPGs as a subclass of movement primitives that can be activated individually or in sequence.

In summary, both CPGs and DMPs are inspired by biological control strategies and offer modular, adaptable frameworks for generating complex movements. Their structural similarities and intrinsic flexibility make them particularly effective for locomotion in robotic systems. These approaches have therefore attracted growing interest in wearable robotics, and this review analyses how they have been implemented in practice.

3. Literature search methodology

A systematic search was conducted in the PubMed, IEEE Xplore, and Scopus online databases to identify articles where CPGs and/or DMPs were applied to exoskeletons or orthoses for locomotion. The search expression included three main topics: Topic = (“Central pattern generator” OR CPG OR “Dynamic Movement Primitives” OR DMP) AND Topic = (Walk* OR Gait OR Locomotion) AND Topic = (Exos* OR Ortho* OR Device). Minor adaptations were made to comply with each database’s specific requirements.

The search was performed from October 2, 2023, to December 12, 2023, without any restriction on publication year. The queries returned 143 articles from PubMed, 88 from IEEE Xplore, and 290 from Scopus, for a total of 521 results. After removing duplicates, 394 articles remained.

Article selection followed the PRISMA 2020 guidelines for systematic reviews, focusing exclusively on database and register searches (Fig. 1). After title screening, studies unrelated to control strategies in exoskeletons or assistive devices were excluded. Abstracts were then reviewed, and additional exclusions were applied. This process yielded 88 articles for full-text assessment.

Final selection was based on the following inclusion criteria: (i) articles written in English, and (ii) presentation of control strategies developed for upper or lower limb exoskeletons. Review articles were excluded, as the aim was to identify original research describing implemented control strategies and their validation.

The selected studies primarily focused on developing control frameworks using CPGs and/or DMPs to plan locomotion in wearable devices. One article lacked detailed information about the control system due to its focus on user evaluation; in this case, an earlier publication describing the control implementation in the same device was included to supplement the analysis. Although the search considered both upper and lower limb devices, all selected studies applied bio-inspired control to lower limb joints.

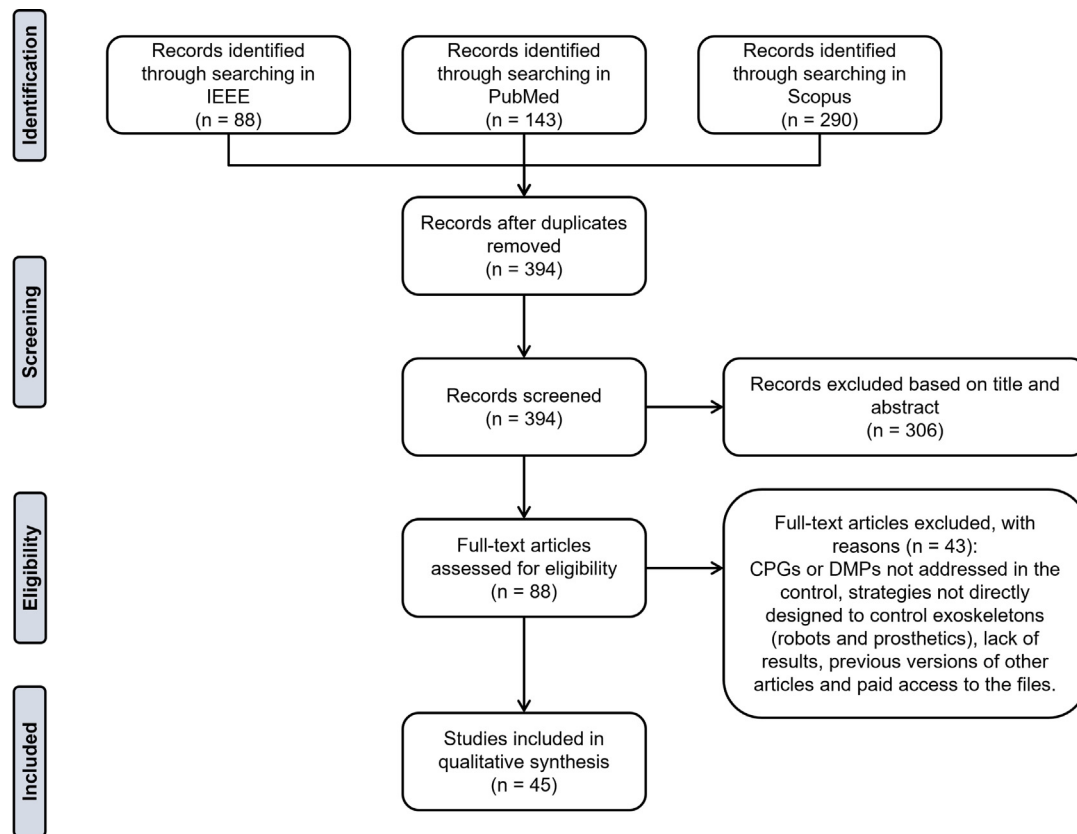


Fig. 1. PRISMA flow chart.

4. Results

After careful screening of the included literature, 45 articles and conference proceedings were included in this review. Of these, 57.8% implemented control strategies using CPGs, while 42.2% employed DMPs. One article ([Wang, Chen, Dong, Du, Shen, & Zhao, 2019](#)) implemented DMPs and used an oscillator to regulate the primitives for each individual leg.

This section presents the results of the systematic review, organized according to the key elements addressed in the reviewed papers. These include the purpose of using CPGs and DMPs in wearable robots, the types of devices and joints involved, the sensors used for modulation and feedback, and the constitution or formulation of the implemented bio-inspired methods. We also describe the techniques adopted to decode user intention, the tracking controllers applied, and the validation procedures employed.

4.1. Citation metrics analysis

To highlight the impact of the strategies analysed in this review, the citation metrics of the selected articles were collected, specifically the number of citations according to CrossRef, as well as the number of full-text reads and downloads (when available from the publishers).

[Table 1](#) summarizes these metrics for each article included in the review.

Among the selected articles, the citation counts varied significantly, ranging from fewer than 5 citations to over 70 citations in well-established studies. To provide a more comprehensive assessment of their impact, a citation-to-readership ratio, which quantifies how frequently a manuscript has been cited relative to its total readership,

was computed. This ratio ranged from 0.12 to 4.7%, with higher values typically observed in studies that introduced innovative CPG and DMP implementations and provided clear experimental validations.

Additionally, it should be noted that more recent studies, despite presenting significant advancements, have not yet had sufficient time to accumulate citations, which may underestimate their long impact.

4.2. Purpose

The use of wearable robotic devices can be divided into three categories: rehabilitation, movement assistance, and power augmentation. Among the articles mentioned, the majority outlined bio-inspired control for rehabilitation (42.2%) and movement assistance (22.2%), or for both (20%). The application of power augmentation was reported in only a small portion of the articles (11.1%), and 2 articles did not restrict the control to a specific application.

[Fig. 2](#) represents the block diagram indicating how CPGs and DMPs were employed in the majority of the articles included in this review. It was identified that the primary objective of the CPG/DMP control block was to generate and sustain rhythmic gait patterns, enabling natural and efficient locomotion across different movement modes. Many implementations adopted a dynamic and adaptive approach, allowing reference patterns to be modulated based on environmental conditions and personalized to meet individual user requirements ([Ahmed et al., 2017](#); [Akbari et al., 2023](#); [Akkawutvanich & Manoonpong, 2023](#); [Chen et al., 2017, 2018](#); [Gui et al., 2017a, 2017b, 2015](#); [Huang et al., 2018, 2019, 2020](#); [Hwang et al., 2021](#); [Mehr et al., 2023, 2021](#); [Sharifi et al., 2021, 2022](#); [Tsukahara et al., 2017](#); [Wang, Tian, Guo, & Wang, 2024](#); [Wang et al., 2022](#); [Xu et al., 2021](#); [Yuan et al., 2019](#); [Zhang et al., 2018](#); [Zhang & Zhang, 2022](#); [Zou et al., 2020](#)).

Table 1

Citation metrics per article included in the review (FTRD: Full-Text Reads and Downloads; N/A: Not Available).

Article	Year	Citations	FTRD	Cit/FRTD (%)
Duvinage, Jiménez-Fabián, Castermans, Verlinden, and Dutoit (2011)	2011	4	303	1.32
Fang, Ren, and Zhang (2014)	2014	14	688	2.03
Ren and Zhang (2014)	2014	16	1009	1.59
Ren and Zhang (2014)	2015	1	167	0.60
Gui, Ren, and Zhang (2015)	2015	4	480	0.83
Gui, Liu, and Zhang (2017a)	2017	19	696	2.73
Gui, Liu, and Zhang (2017b)	2017	71	3256	2.18
Schrade, Nager, Wu, Gassert, and Ijspeert (2017)	2017	14	1289	1.09
Zhang, Ren, Gui, Jia, and Xu (2017)	2017	34	2100	1.62
Tsukahara et al. (2017)	2017	8	255	3.14
Ahmed, Cheng, Lin, Elhassan, and Omer (2017)	2017	3	411	0.73
Chen, Cheng, Yue, Huang, and Guo (2017)	2017	6	404	1.49
Zhang, Ge, Fu, Chen, Luo, and Hashimoto (2018)	2018	8	N/A	N/A
Luo, Sun, Zhao, Zhang, and Tang (2018)	2018	15	414	3.62
Chen, Cheng, Yue, Huang, Guo, et al. (2018)	2018	26	N/A	N/A
Huang et al. (2018)	2018	56	N/A	N/A
Yingxu et al. (2019)	2019	12	1419	0.85
Yuan, Li, Zhao, and Gan (2019)	2019	49	3627	1.35
Huang, Cheng, Qiu, and Zhang (2019)	2019	83	2972	2.79
Wang et al. (2019)	2019	5	370	1.35
Chen, Wang, Zhang, Chen, Zhao, et al. (2020a)	2020	1	228	0.44
Chen, Wang, Zhang, Chen, Zhao, et al. (2020b)	2020	1	222	0.45
Huang, Wu, Qiu, Cheng, Chen, and Peng (2020)	2020	9	N/A	N/A
Ma, Huang, Chen, Song, and Li (2020)	2020	6	335	1.79
Qiu et al. (2020)	2020	42	2161	1.94
Wang and Wang (2020)	2020	2	282	0.71
Zou, Huang, Qiu, Chen, and Cheng (2020)	2020	16	1668	0.96
Sharifi, Mehr, Mushahwar, and Tavakoli (2021)	2021	36	1859	1.94
Mehr, Sharifi, Mushahwar, and Tavakoli (2021)	2021	21	1253	1.68
Xu, Qiu, Yuan, and Cheng (2021)	2021	6	1000	0.60
Qiu et al. (2021)	2021	6	1200	0.50
Hwang, Sun, Han, and Kim (2021)	2021	13	1405	0.93
Wang, Zhao, Sui, Zhao, and Zhu (2022)	2022	1	450	0.22
Mokhtari, Taghizadeh, and Ghaf-Ghanbari (2022)	2022	6	418	1.44
Sharifi, Mehr, Mushahwar, and Tavakoli (2022)	2022	30	2098	1.43
Plaza et al. (2022)	2022	5	466	1.07
Xu, Huang, Li, and Feng (2022)	2022	1	246	0.41
Zhang and Zhang (2022)	2022	14	299	4.68
Tan, Cao, Zhang, Chen, and Li (2022)	2022	2	377	0.53
Luo et al. (2022)	2022	10	682	1.47
Wang et al. (2023)	2023	2	N/A	N/A
Mehr, Guo, Akbari, Mushahwar, and Tavakoli (2023)	2023	1	782	0.13
Akkawutvanich and Manoonpong (2023)	2023	9	1044	0.86
Akbari, Mehr, Ma, and Tavakoli (2023)	2023	1	N/A	N/A
Eken et al. (2023)	2023	2	206	0.97

Beyond locomotion planning, bio-inspired methods have also been employed for synchronizing hybrid assistance strategies, such as Functional Electrical Stimulation (FES) combined with exoskeletons (Ren & Zhang, 2014; Zhang et al., 2017) (Fig. 3). Additionally, these methods have been utilized to predict movement trajectories for real-time estimation of human torque profiles (Qiu et al., 2020, 2021) (Fig. 4) and to continuously estimate the phase of activities of daily living (Eken et al., 2023) (Fig. 5).

4.3. Devices and DoFs

In the reviewed articles, different authors used distinct exoskeleton or orthoses to validate their proposed methods. Some studies utilized commercial exoskeletons such as the Indego exoskeleton developed by Ekso Bionics (Mehr et al., 2023, 2021; Sharifi et al., 2022), PhoeniX by Ottobock (Luo et al., 2022), Exo-H3 from Technaid S.L. (Akbari et al., 2023), and AIDER developed by Buffalo Robot Tech Co. (Chen et al., 2017; Xu et al., 2021; Zou et al., 2020). Other researchers validated the effectiveness of their control strategies by testing them on lower-limb prototypes they had developed themselves. This includes the HUALEX developed by PRMI Lab (Ahmed et al., 2017; Huang et al., 2018, 2019), the WAP-2 (Hwang et al., 2021), the

Curara device developed by Shinshu University (Tsukahara et al., 2017; Zhang et al., 2018), the FEXo Knee (Ren & Zhang, 2014; Zhang et al., 2017), the Hip Assist Exoskeleton-HAE (Qiu et al., 2020, 2021), the Parallel Exoskeleton-prototype PALExo (Wang et al., 2022), and other prototypes developed in university research centres. Fig. 6 shows some of the lower limb exoskeletons used in the various control articles.

Regarding the number of joints in these systems, most of them feature four active joints in the hips and the knees. A few systems reported having six active DoFs, incorporating active ankle joints (Akbari et al., 2023; Akkawutvanich & Manoonpong, 2023). Two articles focused on aiding solely the hip joints using the HAE (Qiu et al., 2020, 2021), while two others provided assistance only to the knee joint (Ren & Zhang, 2014; Zhang et al., 2017). Additionally, one article applied assistance exclusively to the ankle joint using an orthosis (Duvinage et al., 2011).

In terms of joint types, most of them were rotational joints, except for PALExo, which has two prismatic joints per leg (Wang et al., 2022). The joints facilitated movement primarily in the sagittal plane, with one study incorporating an active hip DoF in the frontal plane (Xu et al., 2022). In addition to active DoFs, most devices also include passive DoFs, either at the hip (Ahmed et al., 2017; Huang et al., 2018, 2019; Tsukahara et al., 2017; Zhang et al., 2018), the ankle (Chen et al., 2017; Gui et al., 2017a, 2017b, 2015; Hwang et al., 2021; Luo et al., 2022; Plaza et al., 2022; Xu et al., 2022, 2021; Yuan et al., 2019;

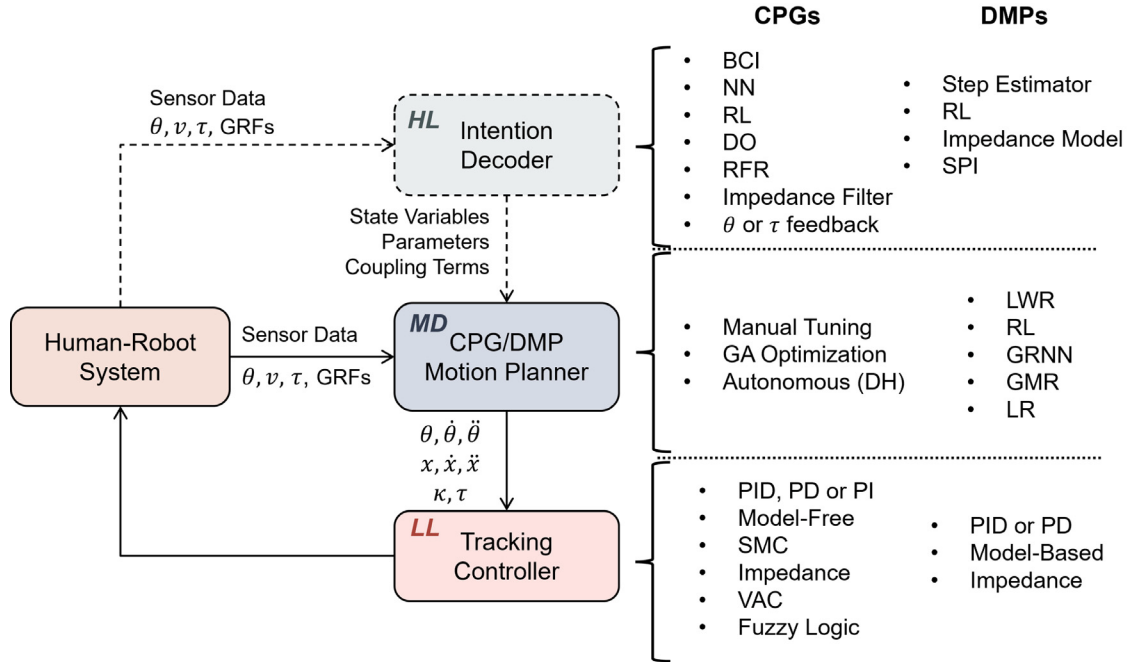


Fig. 2. Generic diagram of bio-inspired control methods. The dashed lines and blocks indicate components that were not included in all strategies. HL — High Level, MD — Middle Level, and LL — Low Level. θ indicates angular position, x indicates position in Cartesian space, v indicates linear velocity, κ indicates stiffness and τ indicates torque. BCI: Brain Computer Interface; NN: Neural Network; RL: Reinforcement Learning; DO: Disturbance Observer; RFR: Random Forest Regression; SPI: Stability Pyramid Index; GA: Genetic Algorithm; DH: Dynamic Hebbian; LWR: Locally Weighted Regression; GRNN: Global Regression Neural Network; GMR: Gaussian Mixture Regression; LR: Linear Regression; SMC: Sliding Mode Control ; VAC: Variable Admittance Control; PID: Proportional-Integral-Derivative; GRFs: Ground Reaction Forces.

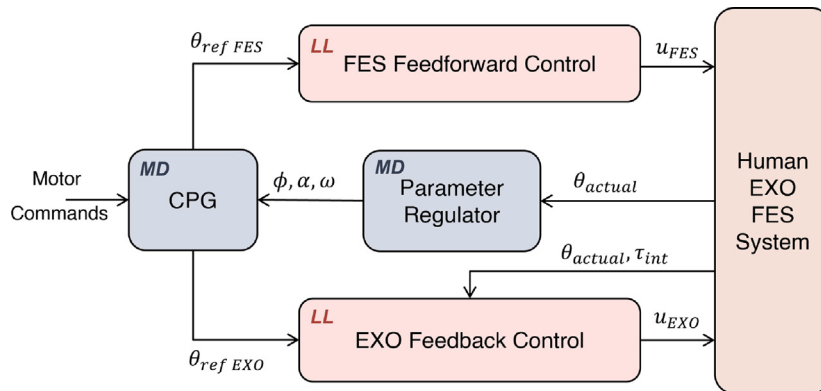


Fig. 3. Cooperative CPG control scheme for synchronizing FES and exoskeleton assistance, as proposed in Ren and Zhang (2014), Zhang et al. (2017).

Zhang & Zhang, 2022; Zou et al., 2020), or both (Wang et al., 2022), whereas the knee was consistently found to be actively controlled. Passive movement in the sagittal or frontal planes was just introduced to enhance mobility and improve the overall user experience.

4.4. Sensors

This section explores the sensors used in the reviewed articles, either to provide feedback for control or as tracking information for validation purposes.

Fig. 7 summarizes all the sensors reported in the reviewed articles. Angular position sensors were the most used, followed by force/pres-
sure sensors. Rotary encoders embedded in the motors were predom-
inantly used to measure joint angles, though hall sensors (Xu et al.,
2022; Yuan et al., 2019), inclinometers (Ahmed et al., 2017; Huang

et al., 2019; Wang et al., 2019), and Inertial Measurement Units (IMUs) (Qiu et al., 2020, 2021) were also found.

Many studies implemented force/pressure sensors for two main purposes: to measure interaction forces between the user and the exoskeleton (Mokhtari et al., 2022; Qiu et al., 2020; Ren & Zhang, 2014; Zhang et al., 2017), or as plantar sensors to capture foot contact information (Ahmed et al., 2017; Akkawutvanich & Manoonpong, 2023; Chen et al., 2017, 2020a, 2020b; Duvinage et al., 2011; Eken et al., 2023; Huang et al., 2018, 2019, 2020; Luo et al., 2022; Mehr et al., 2021; Plaza et al., 2022; Qiu et al., 2020, 2021; Schrade et al., 2017; Xu et al., 2021; Zhang et al., 2018; Zou et al., 2020). Force sensors were applied around the shank (Ren & Zhang, 2014; Zhang et al., 2017) and thigh (Mokhtari et al., 2022; Qiu et al., 2020) to measure interaction forces, while Wang et al. (2019) used gas sensors to collect human–robot interaction (HRI) forces. Plantar sensors were primarily used to measure ground reaction forces (Plaza et al., 2022;

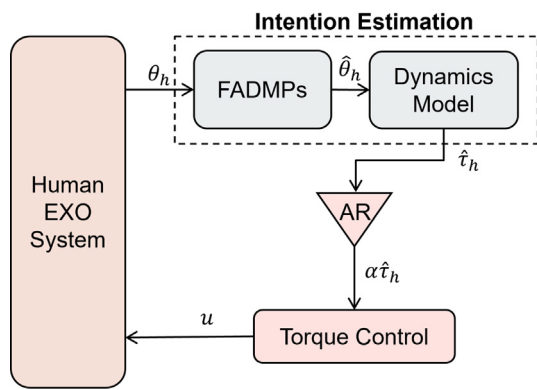


Fig. 4. Frequency Adaptive DMPs for human trajectory prediction, as proposed in Qiu et al. (2020, 2021). AR indicates Assistance Ratio.

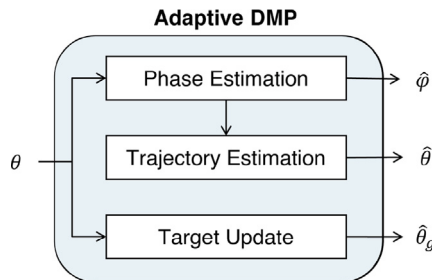


Fig. 5. Adaptive DMPs for continuous phase estimation, as proposed in Eken et al. (2023).

Qiu et al., 2021; Schrade et al., 2017), estimate the Center of Pressure (CoP) and/or Center of Gravity (CoG) (Chen et al., 2020a; Zou et al., 2020), provide phase information for a reference oscillator (Chen et al., 2020b), and detect the phase of motion and gait events such as toe-off (TO) and heel-strike (HS) (Akkawutvanich & Manoonpong, 2023; Duvinage et al., 2011; Eken et al., 2023; Huang et al., 2018; Luo et al., 2022; Mehr et al., 2021; Qiu et al., 2020; Zhang et al., 2018). Wang et al. (2019) incorporated 1D force sensors in the user's shoes to measure vertical ground reaction forces (vGRF) as a comprehensive indicator of the load borne by the wearer. In another approach Chen et al. (2017), pressure sensors were placed on the base of walking sticks to measure contact forces between the stick and the ground. In Huang et al. (2020), the authors used pressure measurements on crutches as an evaluation metric for the control strategy, where lower pressure values were associated with more comfortable physical interaction for the user.

Regarding motion sensors, thirteen articles implemented IMUs for various purposes, including walking velocity measurement (Huang et al., 2018, 2020; Hwang et al., 2021; Plaza et al., 2022; Xu et al., 2021; Zou et al., 2020), posture estimation (Huang et al., 2020; Zou et al., 2020), torso inclination measurement (Huang et al., 2020; Hwang et al., 2021; Luo et al., 2022; Schrade et al., 2017; Xu et al., 2021), estimation of human Centre of Mass (CoM) state (Qiu et al., 2020; Zou et al., 2020), distance measurement (Tan et al., 2022), and computation of orientation angles of the thigh segments (Eken et al., 2023) and of the arm (Chen et al., 2017). Additionally, Huang et al. (2018) used a simple accelerometer to measure the user's walking velocity.

Torque sensors were implemented to detect the human–robot interaction torque between the wearer's movements and the device (Akbari et al., 2023; Tsukahara et al., 2017; Wang et al., 2024; Zhang et al., 2018), or were built into the motors to measure output torque directly (Akkawutvanich & Manoonpong, 2023; Plaza et al., 2022).

Electromyography (EMG) sensors were used for human joint torque estimation as an indicator of motion intention (Gui et al., 2017a, 2017b), and to measure muscle activity for evaluating the controller's effectiveness (Akkawutvanich & Manoonpong, 2023; Qiu et al., 2021). Additionally, Brain–Computer Interfaces (BCIs) utilizing electroencephalogram (EEG) sensors were employed to control rehabilitative exoskeletons and assess cognitive human–robot interaction (cHRI) (Gui et al., 2017b, 2015).

4.5. Central pattern generators

Table 2 resumes the main characteristics of CPGs from the articles endorsed by this review. CPGs were mainly used to produce angular position trajectories in the joint space, except for three articles (Chen et al., 2020a; Gui et al., 2017a; Schrade et al., 2017). In Chen et al. (2020a), the CPG produced driving torques for the extension and flexion muscles of each Schrade et al. (2017) changed the CPG's dynamics to produce a torque reference and included two additional neurons to generate adequate stiffness for the knee joints. Gui et al. (2015) used the CPG to produce not only joint angular positions, but also velocities and accelerations.

CPGs architectures were primarily modelled using neuron-based and non-linear oscillator models. The most commonly implemented oscillating units included the phase oscillator and its variants (Akbari et al., 2023; Chen et al., 2020b; Gui et al., 2017a, 2017b, 2015; Mehr et al., 2023, 2021; Sharifi et al., 2021, 2022; Wang et al., 2024; Zhang et al., 2017), followed by Matsuoka's neuron model (Chen et al., 2020a; Fang et al., 2014; Luo et al., 2018; Ren & Zhang, 2014; Schrade et al., 2017; Tsukahara et al., 2017; Wang et al., 2022; Zhang et al., 2018), the Hopf harmonic oscillator (Ahmed et al., 2017; Duvinage et al., 2011; Mokhtari et al., 2022; Plaza et al., 2022), and Van der Pol's relaxation oscillator (Ajayi et al., 2015). The general equations that describe how these oscillators behave are given in [Appendix B](#).

Despite the diversity of oscillating units, most articles did not explain their selection criteria. Moreover, even studies using the same oscillator type often presented modified equations, incorporating coupling terms or other adjustments to adapt CPG dynamics for specific control behaviours.

A distinct example is a two-layer network CPG introduced by Akkawutvanich and Manoonpong (2023) for controlling a rehabilitative exoskeleton. This architecture featured a rhythmic pattern generation unit with frequency adaptation and a post-processing unit with pattern adaptation. However, no articles described hybrid CPGs.

The number of oscillators per CPG varied depending on the complexity of the desired control signals. For Matsuoka oscillators, most studies utilized two neurons per DoF to simulate joint extension and flexion, as in [Fig. 8\(a\)](#), though one study employed four neurons for the knee joint (Fang et al., 2014). For phase oscillators, configurations ranged from two oscillators per DoF (Gui et al., 2017a, 2017b, 2015; Zhang et al., 2017), while others used five (Chen et al., 2020b) or eight (Akbari et al., 2023; Sharifi et al., 2021, 2022). The CPG presented in [Fig. 8\(b\)](#) controls two DoF using two phase oscillators for each. Hopf oscillators were typically used in networks of five, though one study used seven to control each joint (Mokhtari et al., 2022). An example of two CPGs with Hopf oscillator networks connected together is shown in [Fig. 8\(c\)](#). Similarly, Van der Pol oscillators were organized into a network of four units to control two joints per each leg in Ajayi et al. (2015), as in [Fig. 8\(d\)](#).

Achieving synchronization in multi-DoF systems requires analysing the network topology of CPGs. To simultaneously control the knees and hips, three primary topologies have been identified. The most common approach is nearest-neighbour coupling, where each node communicates only with its immediate neighbours (Fang et al., 2014; Gui et al., 2017a, 2017b, 2015; Luo et al., 2018; Mehr et al., 2023, 2021; Mokhtari et al., 2022; Plaza et al., 2022; Schrade et al., 2017; Sharifi et al., 2022), as illustrated in [Fig. 9\(a\)](#). Another method involves fully interconnected

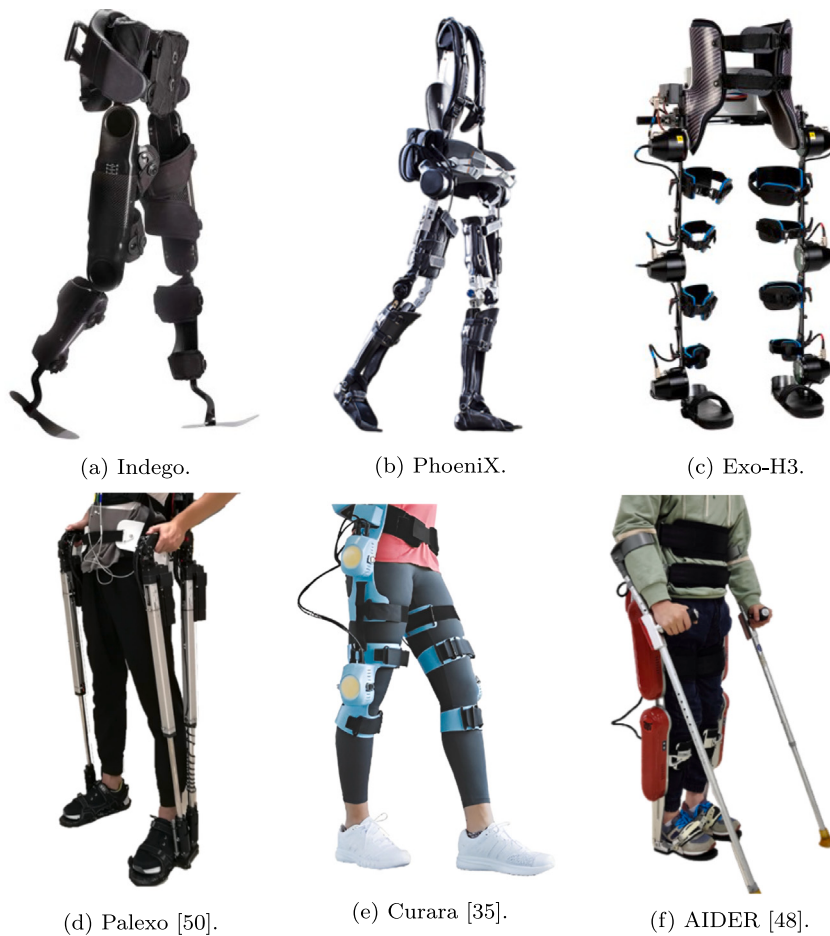


Fig. 6. Lower limb exoskeletons.

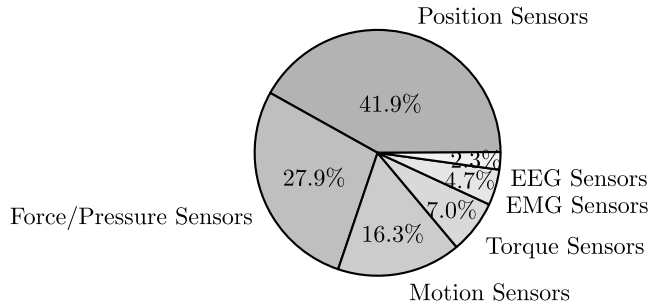


Fig. 7. Distribution of sensor categories.

networks, where all nodes are directly linked (Chen et al., 2020a; Wang et al., 2022; Zhang et al., 2018), as shown in Fig. 9(b). A few studies have employed a different approach (hybrid) depicted in Fig. 9(c), where both knees are also connected as (Ajayi et al., 2015; Fang et al., 2014).

Several studies have incorporated CPGs into LfD frameworks. AFOs were employed in six studies (Ahmed et al., 2017; Chen et al., 2020b; Duvinage et al., 2011; Mokhtari et al., 2022; Plaza et al., 2022; Yingxu et al., 2019), and Fig. 10 illustrates the configuration of the AFOs that form a CPG, derived from the aforementioned sources. The learning phase took place either offline or online. Offline training involved pre-training the CPG using kinematic trajectories from databases or directly collected from users, allowing for consistent pattern replication during assistance sessions without requiring real-time feedback (Duvinage et al., 2011; Plaza et al., 2022; Yingxu et al., 2019). Alternatively,

online learning enabled real-time adaptation by continuously integrating feedback to adjust to changes in user or device movement patterns (Ahmed et al., 2017; Chen et al., 2020b; Mokhtari et al., 2022).

CPGs were also integrated into optimization frameworks to determine parameters like gains, connection weights, and coupling terms. Manual parameter tuning was prevalent, though some studies applied optimization algorithms such as Genetic Algorithms (GA), commonly used for Matsuoka oscillators (Fang et al., 2014; Schrade et al., 2017; Wang et al., 2022), and Harmonic Search Algorithms (HSA) (Mokhtari et al., 2022). To reduce the complexity of the optimization process, many studies adopted simplifications and assumptions, allowing only a limited subset of parameters to be optimized. Symmetry assumptions and the establishment of upper and lower parameter bounds were among the strategies employed in the reviewed articles.

CPG implementations were categorized into open-loop and closed-loop approaches. Open-loop systems generated fixed gait patterns based on predefined parameters without online modulation. These CPGs were often used to generate reference trajectories from previously collected gait data (Ajayi et al., 2015; Fang et al., 2014; Luo et al., 2018; Yingxu et al., 2019). In contrast, closed-loop systems incorporated feedback from the user and the environment, enabling real-time adjustments to amplitudes, frequencies, and phase relationships (Akbari et al., 2023; Chen et al., 2020a, 2020b; Gui et al., 2017a, 2017b, 2015; Mehr et al., 2023, 2021; Schrade et al., 2017; Sharifi et al., 2021, 2022; Tsukahara et al., 2017; Wang et al., 2024, 2022; Zhang et al., 2018, 2017). The closed-loop design is especially advantageous for adaptive strategies.

An example of feedback integration is the use of phase-resetting mechanisms to synchronize exoskeleton movements with human gait. Ground reaction force (GRF) data was commonly used for this purpose,

Table 2
Articles that implemented CPG control.

Author (Year)	Osc. Type	Device	Dof's	Architecture	Feedback	Output
Duvinage et al. (2011)	Hopf	Ankle Orthose	Ankle	5 osc per joint	GRF	Angular Position
Fang et al. (2014)	Matuoka	LLE Prototype	Hips and Knees	2 osc for the hip 4 osc for the knee	N/A	Angular Position
Ren and Zhang (2014)	Matuoka	FEXO Knee	Knee	2 neurons per joint	Joint Angles	Angular Position
Ajayi, Djouani, and Hamam (2015)	Van der Pol	Biped Model	Hips and Knees	network of 4 osc	N/A	Angular Position
Gui et al. (2015)	Sine	LLE Prototype	Hips and Knees	2 osc per joint	BCI	Angular Position
Gui et al. (2017a)	Sine	LLE Prototype	Hips and Knees	3 sets of nodes, each with 8 osc (2 per joint)	HRI Torque	Position Velocity Acceleration
Gui et al. (2017b)	Sine	LLE Prototype	Hips and Knees	2 osc per joint	BCI and HRI Torque	Angular Position
Schrade et al. (2017)	Matuoka	VariLeg Model	Hips and Knees	2 osc for the hip 4 osc for the knee	Joints Angles and GRF	Torque Stiffness
Tsukahara et al. (2017)	Matuoka	Curara	Hips and Knees	2 neurons per joint	HRI Torque	Angular Position
Ahmed et al. (2017)	Hopf	HUALEX	Hips and Knees	N/A	GRF	Angular Position
Zhang et al. (2017)	Phase	FEXO Knee	Knee	2 osc per joint	Joints Angles	Angular Position
Zhang et al. (2018)	Matuoka	Curara	Hips and Knees	2 neurons per joint	HRI Torque	Angular Position
Luo et al. (2018)	Matuoka	LLE Model	Hips and Knees	2 neurons per joint	N/A	Angular Position
Yingxu et al. (2019)	Hopf	LLE Prototype	Hips and Knees	5 osc per joint	N/A	Angular Position
Chen et al. (2020a)	Matuoka	LLE Prototype	Hips and Knees	2 neurons per joint	Torque	Torque
Chen et al. (2020b)	Phase	LLE Prototype	Hips and Knees	5 osc for the hip 2 osc for the knee	GRF	Angular Position
Sharifi et al. (2021)	Phase	Indego	Hips and Knees	8 osc per joint	HRI Energy	Angular Position
Mehr et al. (2021)	Phase	Indego	Hips and Knees	N/A	HRI Energy	Angular Position
Wang et al. (2022)	Matsuoka	PALEXO	Hips and Knees	2 neurons per joint	Joints angles and GRF	Angular Position
Sharifi et al. (2022)	Phase	Indego	Hips and Knees	8 osc per joint	HRI Energy	Angular Position
Mokhtari et al. (2022)	Hopfield	LLE Model	Hips, Knees, Ankles, Waist	7 osc per joint	HRI Force	Angular Position
Plaza et al. (2022)	Hopf	LLE Prototype	Hips and Knees	5 osc per joint	GRF	Angular Position
Wang et al. (2024)	Phase	LLE Model	Knee	N/A	HRI Torque	Angular Position
Mehr et al. (2023)	Phase	Indego	Hips and Knees	N/A	HRI Energy	Angular Position
Akkawutvanich and Manoonpong (2023)	Author's Proposal	LLE Prototype	Hips, Knees and Ankles	3 osc per hip	Joints Angles	Angular Position
Akbari et al. (2023)	Phase	H3	Hips, Knees and Ankles	8 osc per joint	HRI Energy	Angular Position

enabling synchronization of walking phases with gait events and ensuring consistent movement patterns despite stride variability (Chen et al., 2020b; Duvinage et al., 2011; Plaza et al., 2022; Wang et al., 2022). GRF feedback also enabled phase-specific assistance, such as activating stiffness-generating neurons during the stance phase (Schrade et al.,

2017) or generating control signals for the swing phase (Duvinage et al., 2011).

For adaptive and personalized assistance, feedback beyond phase synchronization is essential. Joint angles, foot contact data, and human–robot interaction (HRI) forces or torques were integrated into

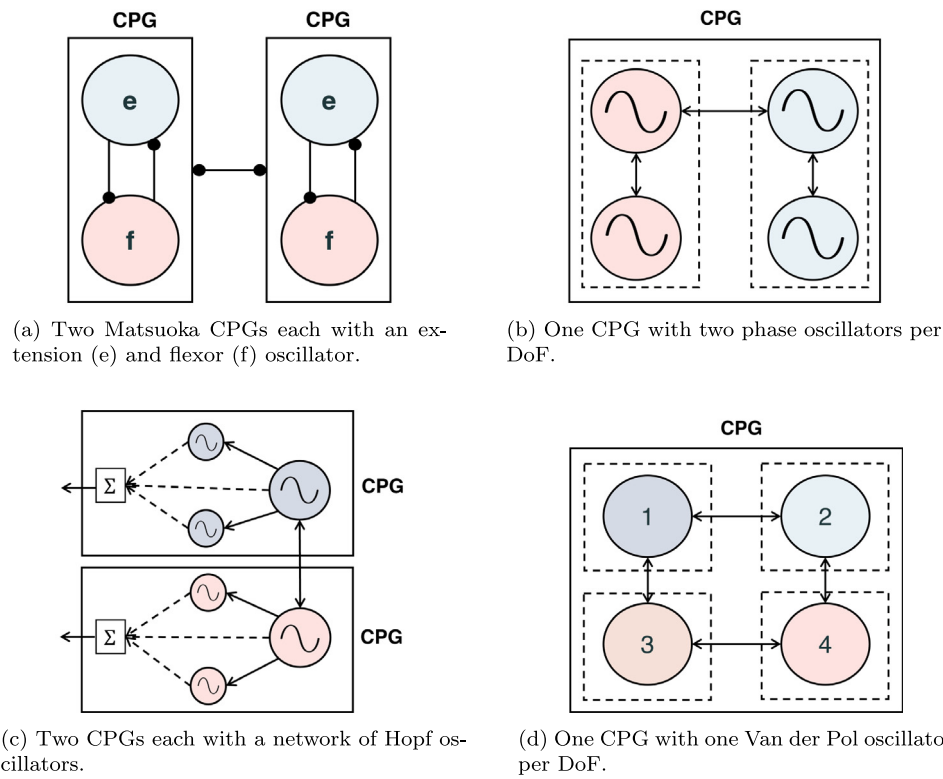


Fig. 8. Examples of CPG networks presented in the articles.

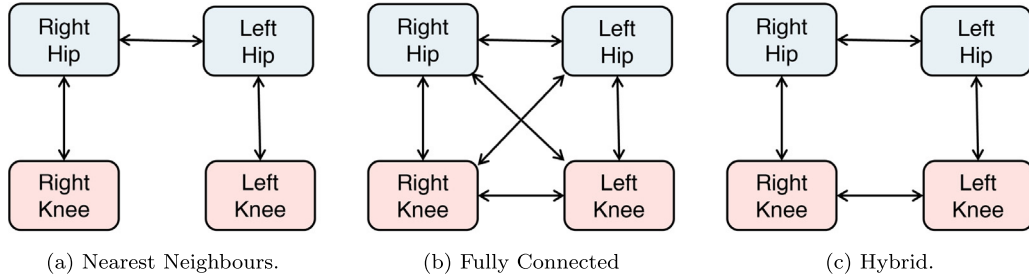


Fig. 9. Topologies adopted for multi-DoF controllers.

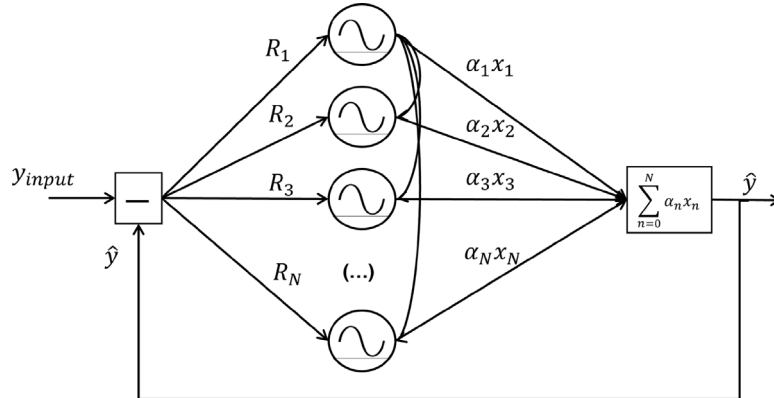


Fig. 10. Adaptive Frequency Oscillators in a network forming a CPG, as in Ahmed et al. (2017), Chen et al. (2020b), Duvinage et al. (2011), Mokhtari et al. (2022), Plaza et al. (2022), Yingxu et al. (2019).

trajectory generation blocks to enable real-time adjustments to the user's needs or environmental conditions. For example, Ahmed et al. (2017) used insole sensor data to adapt walking speed through frequency modulation of CPGs, while Wang et al. (2022) leveraged

GRFs for walking mode recognition and online adjustment of period, amplitude, and phase.

Interaction torques were used in several studies as feedback to excite or inhibit neurons, adjusting variables like frequency, amplitude,

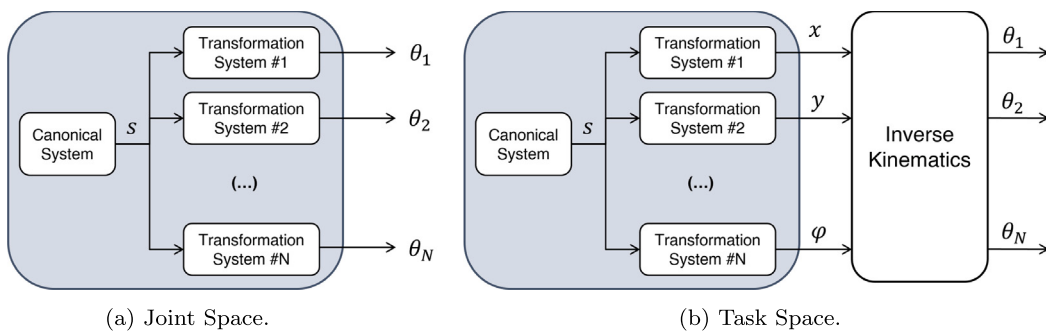


Fig. 11. Motion generation using DMPs.

and phase (Tsukahara et al., 2017; Zhang et al., 2018). Wang et al. (2024) modulated frequency and amplitude based on active torque estimates, while Mokhtari et al. (2022) incorporated interaction forces and Zero Moment Point (ZMP) positions to modulate CPG dynamics. Several studies introduced a novel coupling term based on HRI energy to adjust variables such as frequency, amplitude, and/or equilibrium positions (Akbari et al., 2023; Mehr et al., 2023, 2021; Sharifi et al., 2021, 2022).

Finally, Gui et al. (2015) assigned predefined CPG variables based on movement intention detected using a BCI. A year later, in Gui et al. (2017a), CPG's phase, frequency, and amplitude was updated in real time according to the user's physical effort, measured by EMG data. That same year, an article was published, Gui et al. (2017b), combining both of these modulation approaches with cognitive and physical intention recognition for online adaptation of the CPG.

4.6. Dynamic movement primitives

Table 3 summarizes the main findings of DMP methods applied to exoskeletons and orthoses. DMPs were primarily used to adaptively learn and plan robotic device trajectories based on sensory feedback. However, some studies applied DMPs with alternative approaches. For instance, in Eken et al. (2023), DMPs were incorporated into a continuous gait phase estimation algorithm. In Qiu et al. (2020), bio-inspired control was embedded within a framework for real-time human torque estimation, leveraging sensory data to generate a stable, noise- and delay-free signal.

DMPs dynamically generated joint positions, velocities, and accelerations, with the latter two derivable from the first. These were implemented in both joint space (Eken et al., 2023; Huang et al., 2018, 2019; Hwang et al., 2021; Luo et al., 2022; Ma et al., 2020; Qiu et al., 2020, 2021; Tan et al., 2022; Wang et al., 2019; Wang & Wang, 2020; Xu et al., 2022; Yuan et al., 2019; Zhang & Zhang, 2022) and task space (Chen et al., 2017, 2018; Huang et al., 2020; Xu et al., 2021; Zou et al., 2020). Fig. 11 illustrates the structure of DMPs, where the canonical system provides the time reference for all transformation systems that generate spatial trajectories. The figure distinguishes between trajectory generation directly in joint space and in task space, the latter requiring an additional inverse kinematics block. Notably, no studies were found where DMPs directly generated actuator torques.

A review of the articles revealed that most studies utilized the classical spring-damper model of discrete DMPs. Only three out of nineteen articles implemented limit-cycle oscillator DMPs to model motion trajectories (Huang et al., 2018; Qiu et al., 2020, 2021). In these cases, the trajectory frequency was first estimated, followed by learning the shape of the motion trajectory. For example, Huang et al. (2018) updated the frequency parameter based on the time period of the last recorded gait cycle. Later, Qiu et al. (2020) used an extended Kalman filter to estimate human walking velocity, while another study by Qiu et al. (2020) employed zero-crossing detection for the same purpose.

The remaining studies implemented multi-purpose point attractor DMPs, which modelled gait either on a per-stride basis (Chen et al., 2017, 2018; Huang et al., 2019; Hwang et al., 2021; Luo et al., 2022; Ma et al., 2020; Tan et al., 2022; Wang et al., 2019; Wang & Wang, 2020; Xu et al., 2022, 2021; Yuan et al., 2019), only during the swing phase (Huang et al., 2020), or by segmenting the gait cycle and applying different DMPs to each segment (Zhang & Zhang, 2022). To address issues of discontinuity and sudden movements at the start of each step, researchers introduced a third term to the classic transformation system. This approach was implemented by Chen et al. (2017, 2018), Ma et al. (2020) and Xu et al. (2021).

Huang et al. (2018) justified the use of discrete DMPs by noting that the ending joint angles varied between gait cycles. Similarly, Luo et al. (2022) observed that stroke patients exhibit variability in foot touchdown, causing changes in initial joint angles at the end of the swing phase, further supporting the preference for discrete DMPs.

Regarding the mathematical formulation of DMPs, the discrete version is described by Eqs. (1) to (3). They include the transformational (Eqs. (1) and (2)) and the canonical components (Eq. (3)), where y is the system output and x is the phase variable.

$$\tau \dot{z} = \alpha(\beta(g - y) - z) + f(x) \quad (1)$$

$$\tau \dot{y} = z \quad (2)$$

$$\tau \dot{x} = \alpha_x x \quad (3)$$

The non-linear term, $f(x)$, is expressed as a linear combination of Radial Basis Functions (RBFs), as in Eq. (4)

$$f(x) = \frac{\sum_{i=1}^N w_i \Psi_i(x)}{\sum_{i=1}^N \Psi_i(x)} \quad (4)$$

The rhythmic variant of DMPs follows a similar structure, replacing the temporal parameter τ with the trajectory's frequency Ω , and the phase variable, denoted as ϕ , is also described by a dynamical system (see Appendix B).

The initial formulation introduced the non-linear forcing function as a first-order term, but this approach was later revised due to its analytical limitations (Ijspeert, Nakanishi, Hoffmann, Pastor, & Schaal, 2013). Most of the reviewed articles adopted the modified version, where the non-linear term is applied to the second-order dynamics of the system, as in Eq. (1). However, the original implementation was observed in two studies (Huang et al., 2018, 2019).

Lfd was implemented in all reviewed studies to encode natural motion trajectories into the non-linear forcing function, ensuring reliable reproduction of these trajectories. The effectiveness of this learning process depended on the complexity of the task and the data characteristics. Fig. 12 presents the structure of the learning process using DMPs. Some models combined DMPs with regression techniques (Huang et al., 2018, 2019; Hwang et al., 2021; Luo et al., 2022; Qiu et al., 2020; Wang & Wang, 2020), or Reinforcement Learning (RL) techniques (Chen et al., 2017; Wang et al., 2019; Yuan et al., 2019; Zhang & Zhang, 2022). The most common implemented regression model was Locally Weighted Regression (LWR) (Huang et al., 2018, 2019, 2020; Hwang

Table 3
Articles that implemented DMP control.

Author (Year)	Formulation	Device	DoFs	Feedback	Output
Chen et al. (2017)	Discrete	AIDER	Hips and Knees	GRF	Position
Chen et al. (2018)	Discrete	Human Model	Hips and Knees	GRF and Upper Body Movement	Position
Huang et al. (2018)	Periodic	HUALEX	Hips and Knees	Joints Angles	Angular Position
Huang et al. (2019)	Discrete	HUALEX	Hips and Knees	Joints Angles	Angular Position
Wang et al. (2019)	Discrete	LLE Prototype	Hips and Knees	Joints Angles and GRF	Angular Position
Yuan et al. (2019)	Discrete	LLE Prototype	Hips and Knees	Joints Angles	Angular Position
Zou et al. (2020)	Discrete	AIDER	Hips and Knees	Joints Angles, GRF and Upper Body Movement	Position
Huang et al. (2020)	Discrete	AIDER	Hips and Knees	GRF and Upper Body Movement	Angular Position
Ma et al. (2020)	SDMPs	N/A	Hips and Knees	Joints Angles	Angular Position
Wang and Wang (2020)	Discrete	N/A	Hips and Knees	N/A	Angular Position
Qiu et al. (2020)	Periodic	HAE	Hips	Joints Angles and GRF	Angular Position
Qiu et al. (2021)	Periodic	HAE	Hips	Joints Angles and HRI Torque	Angular Position
Xu et al. (2021)	Discrete	AIDER	Hips and Knees	Joints Angles, GRF and Upper Body Movement	Position
Hwang et al. (2021)	Discrete	WAP-2	Hips and Knees	Joints Angles, Velocity and Inclination	Angular Position
Xu et al. (2022)	Discrete	LLE Prototype	Hips and Knees	Joints Angles	Angular Position
Zhang and Zhang (2022)	Discrete	LLE Prototype	Hips and Knees	Joints Angles	Angular Position
Tan et al. (2022)	Discrete	N/A	Knee	Joints Angles	Angular Position
Luo et al. (2022)	Discrete	PhoeniX	Hips and Knees	N/A	Angular Position
Eken et al. (2023)	aDMPs	N/A	N/A	Joints Angles and GRF	Angular Position

et al., 2021; Luo et al., 2022; Qiu et al., 2020; Wang & Wang, 2020). Other regression methods included the Global Regression Neural Network (GRNN) (Wang & Wang, 2020), Gaussian Mixture Regression (GMR) (Xu et al., 2022), and Linear Regression (LR) (Ma et al., 2020). Wang et al. (2019) compared GRNN with two other learning methods in simulations and found it exhibited superior learning ability and faster convergence towards the desired joint trajectory.

Similar to CPGs, DMPs were implemented in either open-loop or closed-loop configurations. Open-loop setups, observed in three studies, involved pre-teaching reference patterns to DMPs, which then generated only baseline movements during operation (Luo et al., 2022; Tan et al., 2022; Wang & Wang, 2020). Conversely, closed-loop implementations integrated DMPs into negative feedback loops, continuously adapting movements to environmental and user-specific conditions (Chen et al., 2017, 2018; Eken et al., 2023; Huang et al., 2018, 2019, 2020; Hwang et al., 2021; Ma et al., 2020; Qiu et al., 2020, 2021; Wang et al., 2019; Xu et al., 2022, 2021; Yuan et al., 2019; Zhang & Zhang, 2022; Zou et al., 2020).

The feedback signals used in these studies included: (i) joint angles (Eken et al., 2023; Huang et al., 2018, 2019; Hwang et al., 2021; Ma et al., 2020; Qiu et al., 2020, 2021; Tan et al., 2022; Wang et al., 2019; Xu et al., 2022, 2021; Yuan et al., 2019; Zhang & Zhang, 2022; Zou et al., 2020); (ii) ground reaction forces from the user and crutches (Chen et al., 2017, 2018; Eken et al., 2023; Huang et al., 2020; Qiu et al., 2020; Wang et al., 2019; Zou et al., 2020); (iii) upper body movement (velocity and inclination of the torso) (Chen et al., 2018; Hwang et al., 2021; Xu et al., 2021; Zou et al., 2020).

One study implemented phase-resetting via heel strike (HS) detection from GRFs, using a reference oscillator to synchronize DMP patterns with the user (Wang et al., 2019).

The studies demonstrated that DMPs were modulated online at temporal and spatial levels by adjusting the timing parameters, altering the goal, or modifying the non-linear term. Some articles focused solely on amplitude modulation (Chen et al., 2017; Huang et al., 2018; Yuan et al., 2019), while others adjusted both amplitude and frequency to meet specific control requirements (Chen et al., 2018; Huang et al.,

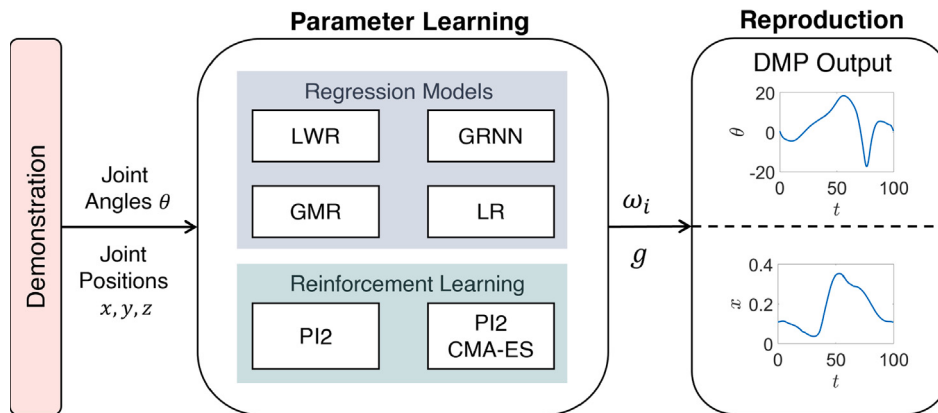


Fig. 12. Learning from demonstration using DMPs.

2019, 2020; Hwang et al., 2021; Ma et al., 2020; Qiu et al., 2020, 2021; Xu et al., 2021; Zou et al., 2020).

Chen et al. (2017) continuously adapted trajectory goals to modify step lengths. Similarly, Chen et al. (2018) adjusted both goal and timing parameters to enhance gait. Other studies used similar strategies for adapting gait to environmental conditions (Hwang et al., 2021) and for balance control (Xu et al., 2021).

Several studies continuously learned the weights of the non-linear term to adapt trajectories to varying slopes (Huang et al., 2020; Zou et al., 2020) or to individual user needs (Huang et al., 2018; Qiu et al., 2020, 2021; Wang et al., 2019; Zhang & Zhang, 2022). Yuan et al. (2019) also employed this method while dynamically adjusting the goal through RL algorithms.

Unlike these methods, Huang et al. (2019) introduced an impedance model as a coupled term in the DMP to produce a trajectory that takes into account the physical interactions between the user and the device.

Finally, Ma et al. (2020) proposed a novel approach that combined multiple pre-learned trajectories and scaled them temporally to generate gait patterns suitable for a wide range of walking speeds.

4.7. Decoding motion intention

Decoding the user's movement intention is a function managed by the high-level perception layer. However, some studies bypassed this layer, instead relying on predefined trajectories for motion generation. In applications such as motion assistance and power augmentation, where users retain control over their movements, generating responsive assistance is essential. Accurately interpreting the user's intentions and needs is therefore critical. The reviewed articles addressed this challenge using two main approaches: cognitive decoding and interpretation of physical interactions.

Cognitive decoding leverages direct neural signals to interpret user intent. For example, Gui et al. (2015) developed online Brain–Computer Interfaces (BCIs) that use EEG signals to reflect the user's intentions in real-time.

Decoding physical interactions involves interpreting the forces or movements generated during Human–Robot Interaction (HRI). Interaction torques or forces, often referred to as HRI metrics, serve as indicators of human intent as they reflect the user's applied forces.

HRI torque can be measured directly using built-in torque sensors. For instance, Zhang et al. (2018) calculated interaction torque by subtracting a gravity compensation term from the measured torque. Similarly, Tsukahara et al. (2017) used torque sensors to measure the voluntary motion of the wearer relative to the device as input for trajectory planning. Mokhtari et al. (2022) adjusted desired trajectories by minimizing interaction forces, calculated as the difference between desired and measured forces through an impedance filter.

Since direct measurement of interaction torque can be challenging, several studies proposed estimation methods. For example, Huang et al. (2018) introduced an impedance model based on angular position and velocity differences between the user and the exoskeleton for online gait adjustment.

Electromyography (EMG) data also offers a way to estimate interaction torque. Gui et al. (2015) used EMG signals to estimate knee joint torque, which was then converted into state variables for trajectory adjustments. Identically, Gui et al. (2017b) employed EMG data to compute physical HRI, enabling precise trajectory adaptation.

Other estimation approaches include the use of Neural Networks (NNs). Sharifi et al. (2021) trained a NARX NN to estimate non-linear passive dynamics using joint position and velocity as inputs, with torque as the output. This enabled accurate calculation of active human torque for real-time trajectory adjustment. Similar methods were implemented by J.K. Mehr et al. in subsequent studies (Mehr et al., 2023, 2021).

Additional methods include Distance Observers (DOs) and Random Forest Regression (RFR). Sharifi et al. (2021) designed a Time-varying Bounded-gain Adaptive (TBA) DO for estimating HRI torque in a CPG-based control framework. Akbari et al. (2023) used RFR to predict passive dynamics from joint position, velocity, and acceleration data, thereby estimating HRI torque to refine gait control signals. Alternatively, Wang et al. (2019) used a non-linear Disturbance Observer (NDO) to estimate user torque from joint trajectory feedback, incorporating this torque directly into CPG equations for motion trajectory adjustments.

Qiu et al. (2020) proposed a real-time estimator for walking intention based on kinematic data, ground reaction forces (GRFs), and human body inertial parameters. By combining a human dynamic model with trajectories generated by DMPs, they estimated torque signals at the hip and knee joints. The same algorithm was later applied to an exoskeleton control framework (Qiu et al., 2021).

Unlike the aforementioned methods, other articles simply used angular position feedback to adapt trajectories to users' needs. Luo et al. (2022), used joint feedback and a "lookahead distance" parameter to adjust trajectories generated by DMPs. Akkawutvanich and Manoonpong (2023) indirectly inferred user intention from leg movement frequency, enabling rapid online adaptation of personalized gaits. Huang et al. (2018) utilized the error between the reference trajectory and the actual trajectory executed by the exoskeleton to detect changes in gait patterns. The adjustment process involved continuously recording and learning new trajectories whenever the user altered their movement pattern.

GRFs were another key metric for decoding user intention. Ahmed et al. (2017) analysed heel contact timing mismatches between the

user's footwear and the exoskeleton's footboard to determine user intent to accelerate or decelerate. This information was used to calculate a walking speed control parameter for trajectory adaptation.

For paraplegic patients, human intention can also be inferred from upper body movement. Chen et al. (2017) linked user intention to torso inclination and crutch placement, using these cues to adjust step length. Hwang et al. (2021) employed a similar approach to adapt gait patterns based on the wearer's condition.

Finally, an intention estimator for initiating a step, based on an orbital energy diagram, was developed by Chen et al. (2018). By modelling the user's body as a Linear Inverted Pendulum (LIP), they detected shifts in weight distribution to estimate forward or backward step intention.

4.8. Tracking controllers

The low-level controllers are responsible for executing control commands directly on the device, ensuring that it follows the trajectories generated by the high- or mid-level control layers. This section summarizes the approaches used for this layer of control in the reviewed articles.

Proportional-Derivative (PD) and Proportional-Integral-Derivative (PID) controllers were the most commonly employed methods for low-level tracking, although some studies did not specify the method used. Only one study, conducted by Qiu et al. (2020), implemented a Proportional-Integral (PI) controller.

These controllers typically operate by minimizing the error signal between the desired reference and the actual system output. Most articles relied on position error for this purpose, while some opted to minimize torque error (Chen et al., 2018; Gui et al., 2015; Qiu et al., 2020, 2021; Schrade et al., 2017; Sharifi et al., 2022; Wang et al., 2024). In Wang et al. (2022), control was instead based on force error, demonstrating an alternative approach.

The choice of proportional, derivative, and/or integral gains significantly impacts the performance of these controllers. However, the majority of authors did not explicitly explain how they were determined. Among those who did, methods such as trial and error (Gui et al., 2017b; Ren & Zhang, 2014; Zhang et al., 2018, 2017), subject feedback to optimize for stable and comfortable walking (Gui et al., 2017a), and adjustments for rapid and stable joint angle tracking (Zhang et al., 2018) were reported. Zou et al. (2020) indicated the use of a high-gain PID.

Novel low-level controllers were also proposed, such as the model-free controller (TDE-PPMFC) by Wang et al. (2019) and the model-based RL controller used in Huang et al. (2018, 2019). Admittance and impedance controllers were also employed at the low level. In Ahmed et al. (2017), the CPG sends its reference to a variable admittance controller. In Ahmed et al. (2017), Luo et al. (2022, 2018), the low-level control is governed by impedance control laws.

4.9. Validation procedures

Of the 45 selected studies, 34 conducted experimental validation of the control systems with human subjects wearing an exoskeleton or orthosis. Eleven studies validated the control exclusively through simulations (Ajayi et al., 2015; Chen et al., 2018; Duvinage et al., 2011; Hwang et al., 2021; Luo et al., 2018; Ma et al., 2020; Mokhtari et al., 2022; Schrade et al., 2017; Tan et al., 2022; Wang et al., 2024; Wang & Wang, 2020), without extending the theoretical concepts to real-world scenarios.

In the experimental studies, the number of participants was typically small, with most using 12 or fewer subjects and many involving only a single individual operating the device (Ahmed et al., 2017; Akbari et al., 2023; Chen et al., 2017; Hwang et al., 2021; Mehr et al., 2023, 2021; Plaza et al., 2022; Sharifi et al., 2021; Wang et al., 2019, 2022;

Xu et al., 2022; Zhang et al., 2018). These participants were predominantly healthy individuals with no prior disorders, even in studies targeting therapeutic applications. Participants' ages ranged from their twenties to over seventy years, and in studies where gender was reported, over 75% were male. Notable exceptions included validation with specific patient populations, such as two stroke survivors in the work by Gui et al. (2015), 10 patients diagnosed with spinocerebellar degeneration in Tsukahara et al. (2017), and three stroke survivors and one brain-injured patient in Zhang et al. (2018).

Evaluation protocols were tailored according to the study objectives, with flat-ground walking being the most common activity (Ahmed et al., 2017; Akbari et al., 2023; Akkawutvanich & Manoonpong, 2023; Chen et al., 2017; Eken et al., 2023; Huang et al., 2018, 2019; Hwang et al., 2021; Luo et al., 2022; Mehr et al., 2023, 2021; Plaza et al., 2022; Qiu et al., 2020; Sharifi et al., 2021, 2022; Tsukahara et al., 2017; Wang et al., 2019, 2022; Xu et al., 2022; Yuan et al., 2019; Zhang et al., 2018; Zhang & Zhang, 2022). Other reported activities included standing on support plates (Fang et al., 2014; Gui et al., 2017a, 2017b, 2015), treadmill walking (Akkawutvanich & Manoonpong, 2023; Chen et al., 2020a, 2020b; Qiu et al., 2021), seated knee joint movement (Ren & Zhang, 2014; Zhang et al., 2017), walking on inclined surfaces (Eken et al., 2023; Zou et al., 2020) and stair navigation (Eken et al., 2023).

In validation procedures involving walking trials, various conditions were observed. Some studies focused on steady-state locomotion at self-selected, slower, or faster paces (Fang et al., 2014; Luo et al., 2022; Qiu et al., 2020, 2021; Tsukahara et al., 2017; Wang et al., 2019, 2022; Yuan et al., 2019; Zhang et al., 2018; Zhang & Zhang, 2022), while others examined walking during transitions, such as phases of acceleration and deceleration initiated by the user (Ahmed et al., 2017; Akbari et al., 2023; Akkawutvanich & Manoonpong, 2023; Eken et al., 2023; Gui et al., 2017a, 2017b; Huang et al., 2018, 2019; Mehr et al., 2023, 2021; Plaza et al., 2022; Qiu et al., 2021; Sharifi et al., 2021, 2022). One study explored stride length modulation based on the user's intention (Chen et al., 2017).

To ensure safety during walking trials, many studies employed assistive or supportive devices for balance and stability. These included crutches (Akbari et al., 2023; Akkawutvanich & Manoonpong, 2023; Hwang et al., 2021; Luo et al., 2022; Xu et al., 2022; Yingxu et al., 2019; Yuan et al., 2019; Zou et al., 2020), strollers (Mehr et al., 2023; Sharifi et al., 2022; Zhang & Zhang, 2022), fixed or moving platforms attached to the ceiling (Chen et al., 2020a, 2020b; Fang et al., 2014; Gui et al., 2017a; Mehr et al., 2021), and combinations of them (Chen et al., 2017; Luo et al., 2018; Sharifi et al., 2021).

To assess the controllers performance, most articles analysed gait kinematics and kinetics. The most common approach was comparing joint angles with expected trajectory to verify the system's tracking accuracy (Ahmed et al., 2017; Akbari et al., 2023; Akkawutvanich & Manoonpong, 2023; Fang et al., 2014; Gui et al., 2017a, 2017b; Huang et al., 2018, 2019; Hwang et al., 2021; Luo et al., 2022; Mehr et al., 2023, 2021; Plaza et al., 2022; Qiu et al., 2020, 2021; Ren & Zhang, 2014; Sharifi et al., 2021, 2022; Wang et al., 2024; Xu et al., 2022; Yingxu et al., 2019), Mean Absolute Error (MAE) (Akkawutvanich & Manoonpong, 2023; Qiu et al., 2020; Wang & Wang, 2020; Yingxu et al., 2019; Zhang et al., 2017), normalized Mean Square Error (nMSE) (Huang et al., 2018, 2019), and Root Mean Square Error (RMSE) (Luo et al., 2022; Qiu et al., 2021).

In addition to joint angular positions, some studies also reported joint velocities, accelerations, interaction torques, and forces (Eken et al., 2023; Gui et al., 2017a; Huang et al., 2019; Mehr et al., 2023;

Plaza et al., 2022; Qiu et al., 2020; Ren & Zhang, 2014; Sharifi et al., 2022; Wang et al., 2019; Zhang et al., 2018, 2017). Gui et al. (2015) provided details about the time delay between the exoskeleton and the CPG, and Akkawutvanich and Manoonpong (2023) reported the average convergence time for CPG frequency adaptation.

Several studies also analysed muscle activation patterns using EMG data (Akkawutvanich & Manoonpong, 2023; Gui et al., 2017b; Qiu et al., 2021), and metabolic cost measures (Qiu et al., 2021) to assess the device's impact on the wearer. Two studies established a relationship between the intensity of GRFs and user comfort, analysing GRFs and pressure sensed in the crutches (Chen et al., 2017; Wang et al., 2022). Chen et al. (2017) successfully reduced the pressure measured in the sticks by developing a step length adaptation method, which also resulted in a reduction of the pilot's energy cost. Similarly, Wang et al. (2019) compared the decrement ratio (DC) of vertical ground reaction forces (vGRF) with and without the exoskeleton under different load-carrying conditions. To calculate the DC, the average value of the vGRF peak over three gait cycles was measured under various experimental conditions. The authors found that while walking with loads of 25 and 45 kg, the controller enabled the exoskeleton to support the load, reducing the burden on the user.

Differing from these methods, Tsukahara et al. (2017) derived the Harmonic Ratio (HR) from a Fourier analysis of trunk acceleration to quantify walking smoothness, rhythmicity, and stability. Since higher HR values correspond to smoother and more stable motion patterns, the authors concluded that the system improved the wearer's motion in the vertical (V) direction.

For a more comprehensive evaluation, some studies compared the proposed strategy with previously developed methods. Ahmed et al. (2017) compared their modified Variable Admittance Control (VAC) strategy with the traditional VAC method. Wang et al. (2019) contrasted the resultant interaction forces of their proposed approach with the SAC method previously used in power-augmentation exoskeletons. Similarly, Luo et al. (2022) presented results from their suggested control method and compared it with a prior approach they had proposed.

Another important analysis, observed in only a few studies, involved comparing assisted walking with unassisted walking conditions, either without the exoskeleton or with the exoskeleton in zero-torque control, to determine if the device was indeed beneficial to the wearer (Akkawutvanich & Manoonpong, 2023; Luo et al., 2022; Qiu et al., 2021; Tsukahara et al., 2017; Wang et al., 2022).

While some studies report on the comfort experienced by participants, the methodology for collecting such information is often unclear. Typically, comfort is assessed through questionnaires based on participants' subjective perceptions.

5. Discussion

5.1. Applications

CPGs and DMPs bio-inspired approaches were implemented as adaptable and personalized motion generation blocks within the control strategies, forming either the high- or mid-level control blocks, depending on the framework and terminology used by the authors. Their use in exoskeletons and orthoses can be grouped into three main applications, and the strategies proved suitable for all of them. These control methods were incorporated into strategies for speed control, synchronization with the environment, postural stability, stride length adaptation, dynamic balance control (both on level ground and slopes), estimation of walking intention, and gait phase estimation.

While they were primarily used to generate joint angular trajectories adaptively, some studies developed torque and stiffness profiles using CPGs. DMPs encoded trajectories both in joint space and Cartesian space, whereas CPGs were exclusively used to generate trajectories in joint space.

5.2. Joints controlled

CPGs and DMPs were implemented exclusively for lower limb control in the selected articles. During locomotion, the joints of the lower limbs exhibit quasi-periodic behaviour, that is naturally optimized for performing complex tasks with high efficiency and stability. The two bio-inspired control strategies proved suitable for replicating such behaviour in LLE's active joints.

The main actively assisted DoFs were the hip and knee for flexion/extension, followed by the ankle joint for dorsiflexion/plantarflexion. The ankle joint was not actively controlled in most studies and the waist was only mentioned in one article (Mokhtari et al., 2022).

Finally, although one might assume that an increase in controlled DoFs would proportionally enhance the assistance provided, it is important to note that it also significantly increases both the weight of the device and the complexity of the bio-inspired controller. Each additional DoF requires careful tuning of more variables to ensure seamless coordination and fluidity in movement execution, therefore, achieving an optimal balance between these factors is crucial to provide effective assistance.

5.3. Sensors

The categories of sensors detected in the articles were: (i) position; (ii) motion; (iii) force/pressure; (iv) torque; (v) EMG; and (vi) EEG. Angular position sensors were present in almost every article, specifically rotary encoders, potentiometers, hall sensors and inclinometers. Force/pressure sensors were extensively used for two main objectives, measuring interaction forces/torques between the user and the device (Mokhtari et al., 2022; Qiu et al., 2020; Ren & Zhang, 2014; Zhang et al., 2017) and as plantar sensors to provide information on gait events (Ahmed et al., 2017; Akkawutvanich & Manoonpong, 2023; Chen et al., 2018, 2020a, 2020b; Duvinage et al., 2011; Eken et al., 2023; Huang et al., 2018, 2019, 2020; Luo et al., 2022; Mehr et al., 2021; Plaza et al., 2022; Qiu et al., 2020, 2021; Schrade et al., 2017; Xu et al., 2021; Zhang et al., 2018; Zou et al., 2020). Torque (Akbari et al., 2023; Akkawutvanich & Manoonpong, 2023; Plaza et al., 2022; Tsukahara et al., 2017; Wang et al., 2024; Zhang et al., 2018), EMG (Akkawutvanich & Manoonpong, 2023; Gui et al., 2017a, 2017b; Qiu et al., 2021), and EEG sensors (Gui et al., 2017a, 2015) were implemented to detect higher-order commands and modulate the control accordingly. The incorporation of these and other sensors depend on the control features the authors seek to implement. In addition to sensors that provide relevant data for integration into the control loop, additional sensory data can be collected to monitor the condition of both the equipment and the user, which will improve the assessment of the control system performance.

The results collected in this literature review coincide with the ones presented by Sun et al. (2022), in which mechanical sensors are widely used to form complete and powerful measurement systems and EMG and EEG prior signals acquisition is also reported.

Adding too many sensors can increase sophistication, cost, power consumption, and weight. However, there are significant benefits in terms of reliability, accuracy, and robustness. In systems where the human interacts directly with the robot, and the control loop depends on sensory feedback to generate motion – such as with CPG and DMP strategies – redundancy is crucial. Therefore, careful selection of sensors is essential. To avoid the drawbacks of excessive sensor complexity or over-reliance on sensor accuracy, it is important to define the system's requirements clearly, ensuring that only the necessary sensors are chosen to provide the needed information.

5.4. CPG structure

The reviewed articles primarily implemented two types of CPGs: neuron-based models and non-linear oscillator models. Among the former, Matsuoka's unit was broadly implemented, ranking as the second most frequently used approach overall (Chen et al., 2020a; Fang et al., 2014; Luo et al., 2018; Ren & Zhang, 2014; Schrade et al., 2017; Tsukahara et al., 2017; Wang et al., 2022; Zhang et al., 2018). Regarding CPGs with non-linear oscillators, the Phase oscillator emerged as the most widely used (Akbari et al., 2023; Chen et al., 2020b; Gui et al., 2017a, 2017b, 2015; Mehr et al., 2023, 2021; Sharifi et al., 2021, 2022; Zhang et al., 2017), followed by the harmonic Hopf oscillator (Ahmed et al., 2017; Duvinage et al., 2011; Mokhtari et al., 2022; Plaza et al., 2022). The Van der Pol oscillator was found in only one study (Ajayi et al., 2015). Despite the variety of oscillators used, the reviewed articles generally lacked a reason for their selection.

CPG architectures are closely linked to the type of oscillator used and the signals processed by the network. Matsuoka's oscillator's typical architecture involves two neurons per joint to reproduce antagonistic movements, such as flexion and extension. For both Phase and Hopf oscillators, no consistent architecture emerged. In addition, no hybrid CPGs – comprising different types of oscillators within the same network – were found (Yu et al., 2013).

In systems designed to control multiple DoFs, the coupling topologies between CPGs were categorized into fully connected networks, where all oscillators are interconnected, and nearest-neighbour coupling, where oscillators are connected only to their adjacent counterparts.

The structure of a CPG is highly dependent on the specific requirements and constraints of the system it is intended to control. Designing and selecting appropriate oscillatory units, network architectures, and coupling strategies is a non-trivial task, as these elements must be carefully tailored to meet the system's performance metrics and adaptability needs.

5.5. DMP structure

Considering that human locomotion follows a quasi-periodic pattern, one might expect that most of the literature employing DMPs for motion planning in exoskeletons or orthoses would utilize the periodic formulation of DMPs. However, the original formulation of discrete DMPs was most commonly employed across the reviewed articles (Chen et al., 2017, 2018; Huang et al., 2019, 2020; Hwang et al., 2021; Luo et al., 2022; Tan et al., 2022; Wang et al., 2019; Wang & Wang, 2020; Xu et al., 2022, 2021; Zhang & Zhang, 2022). These patterns were typically generated for each step individually, and in some cases, DMPs were not used to model the complete gait cycle. In such instances, careful attention was given to the start and end positions, resulting in a point-to-point attractor. A smaller number of studies implemented periodic DMPs, which enabled continuous joint movement generation throughout the gait cycle (Chen et al., 2020b; Huang et al., 2018; Qiu et al., 2020, 2021).

The rationale behind the choice of DMP formulation was seldom discussed in the articles, with the exception of two studies (Huang et al., 2019; Luo et al., 2022) that justified the use of discrete DMPs due to the larger variance in the initial joint angles during gait cycles. Ultimately, the selection of the appropriate DMP type is driven by the specific application requirements and the desired control granularity. Periodic DMPs are favoured when the objective is to achieve smooth transitions between phases of the gait, offering a more continuous approach to movement generation. Conversely, discrete DMPs are more suitable when the focus is on providing targeted assistance during specific events of the gait cycle, allowing for the decomposition and modelling of individual walking phases.

5.6. Feedback pathways

In the reviewed articles, not all controllers incorporated sensory feedback, with some relying solely on predefined trajectories. While this approach simplifies implementation and reduces system complexity, it inherently limits the controller's adaptability to the user, the device, and environmental changes, thereby not fully exploring the potential of bio-inspired methods.

Several studies addressed these limitations by integrating sensory feedback to enhance control adaptability and responsiveness. Feedback signals commonly used included joint angle feedback (Akkawutvanich & Manoonpong, 2023; Chen et al., 2020a; Eken et al., 2023; Huang et al., 2018, 2019; Hwang et al., 2021; Luo et al., 2018; Ma et al., 2020; Qiu et al., 2020, 2021; Schrade et al., 2017; Wang et al., 2019, 2022; Xu et al., 2022, 2021; Yuan et al., 2019; Zhang et al., 2017; Zhang & Zhang, 2022; Zou et al., 2020), foot contact information (Ahmed et al., 2017; Chen et al., 2017, 2018, 2020b; Duvinage et al., 2011; Eken et al., 2023; Huang et al., 2020; Qiu et al., 2020; Schrade et al., 2017; Wang et al., 2019, 2022; Zou et al., 2020), and human–robot interaction (HRI) torque data (Gui et al., 2017a, 2017b; Tsukahara et al., 2017; Wang et al., 2024; Zhang et al., 2018). The most common strategy involved feeding joint trajectory values directly into the motion generation block, often supplemented by gait event data from foot sensors. These gait events helped reset phases or acted as markers to ensure timely application of control commands.

To improve the transparency of wearable devices and reduce the effort perceived by users, some systems minimized HRI forces by leveraging force or torque data as feedback. This approach proved particularly effective when users applied voluntary adjustments to joint movements, allowing the trajectory to be dynamically altered (Wang et al., 2024). In certain cases, torque feedback was used directly, while other studies introduced the term of HRI energy (Akbari et al., 2023; Mehr et al., 2023, 2021; Sharifi et al., 2021, 2022). These innovations contributed to improved performance and responsiveness, ultimately enhancing the overall user experience.

5.7. Detection of human intention

Decoding human intention is crucial for enabling users to control the movement executed by wearable robotic devices. In wearable robotics, particularly for lower-limb movement, human intention decoding plays a central role. The user's intention has been derived from various sources, including joint angles (Akkawutvanich & Manoonpong, 2023; Huang et al., 2018, 2019; Hwang et al., 2021; Luo et al., 2022; Wang et al., 2019), foot contact information (Ahmed et al., 2017; Mehr et al., 2023), interaction forces and torques (Akbari et al., 2023; Gui et al., 2017a, 2017b; Mehr et al., 2023, 2021; Mokhtari et al., 2022; Qiu et al., 2021; Sharifi et al., 2021, 2022; Tsukahara et al., 2017; Wang et al., 2024), and cognitive commands (Gui et al., 2017b, 2015).

Joint angles, which are voluntarily modulated by the user during movement, have been incorporated into higher-level control blocks, allowing CPGs and DMPs to adapt trajectories based on the user's intentions (Akkawutvanich & Manoonpong, 2023; Huang et al., 2018; Hwang et al., 2021; Luo et al., 2022; Wang et al., 2019). One study utilized foot contact information to develop an algorithm capable of distinguishing the user's intention to accelerate, decelerate, or maintain velocity (Ahmed et al., 2017).

Interaction torque has been measured directly through torque sensors or estimated using various methods, including: (i) neural networks (Mehr et al., 2023, 2021; Sharifi et al., 2021); (ii) random forest regression algorithms (Akbari et al., 2023); (iii) non-linear disturbance observers (Sharifi et al., 2022; Wang et al., 2024); (iv) electromyography (EMG) signals (Gui et al., 2017a, 2017b); and (v) human inverse kinematics (Qiu et al., 2020, 2021). Impedance filters, which calculate the error between desired and actual interaction forces, were also employed, achieving satisfactory results (Mokhtari et al., 2022).

However, decoding intention solely from mechanical sensor feedback has limitations. Users must initiate movement before the device can respond, resulting in delays that affect real-time responsiveness. Additionally, the integration of mechanical sensors introduces technical challenges.

Brain-computer interfaces (BCIs) have demonstrated potential for accurately decoding human movement intentions (Gui et al., 2017b, 2015). However, BCIs require complex signal processing, which increases the transient state duration and introduces significant delays. For example, Gui et al. (2015) achieved a mean recognition rate of 92.4%, but the mean transient state lasted 1.69 s. In a subsequent study, Gui et al. (2015) reported a delay close to 2 s due to electroencephalography (EEG) signal processing and classification algorithms, far exceeding the expected 300 ms delay threshold (Grosse-Wentrup, Mattia, & Oweiss, 2011).

EMG signals also offer promise but present several challenges, such as sensitivity to electrode positioning, muscle fatigue, variable electrode-skin conductivity, and calibration issues, which complicate their application in real-world scenarios (Gantenbein, Dittli, Meyer, Gassert, & Lambery, 2022; Qiu et al., 2021). Mapping EMG signals to joint torque requires biomechanical models customized to the user. Despite these limitations, EMG provides an advantage by detecting muscle activity prior to movement, reducing response delays. Although EEG signals precede EMG in the hierarchy of movement generation by detecting brain activity before muscle activation (Niazi, Jiang, Tiberghien, Nielsen, Dremstrup, & Farina, 2011), EMG remains a valuable tool for preemptive intention decoding.

In conclusion, while challenges remain in fully decoding user intentions, the reviewed methods have demonstrated strong performance in enabling wearable robotic devices to interpret and respond to user intent effectively.

5.8. Low-level tracking controllers

The reviewed literature primarily identifies two methods for low-level control: position control and torque control. Among these, position control is the more commonly used approach due to its simplicity. However, it often lacks compliance and sensitivity, which may limit its effectiveness in certain applications. Torque control, on the other hand, provides greater flexibility and adaptability, but it introduces additional complexity and potential stability challenges. The choice between these two methods depends largely on the specific requirements and constraints of the system.

In most cases, the generation of position or torque references is managed by higher-level control layers, commonly referred to as motion generation or motion learning layers. In this review, these layers often employed strategies such as CPGs or DMPs. To ensure precise trajectory tracking, traditional low-level controllers like PID, PD, and PI were widely utilized (Ahmed et al., 2017; Ajayi et al., 2015; Akkawutvanich & Manoonpong, 2023; Chen et al., 2018; Duvinage et al., 2011; Gui et al., 2017a; Huang et al., 2020; Hwang et al., 2021; Mehr et al., 2023, 2021; Qiu et al., 2021; Ren & Zhang, 2014; Sharifi et al., 2021; Tsukahara et al., 2017; Wang et al., 2019, 2022; Zhang et al., 2018, 2017; Zou et al., 2020).

Beyond these conventional approaches, several studies explored alternative tracking controllers to enhance performance and adaptability. These included impedance and admittance control laws (Ahmed et al., 2017; Luo et al., 2022, 2018; Zhang et al., 2017), novel model-free controllers (Wang et al., 2024), and hybrid approaches that combine model-based control with reinforcement learning (RL) (Huang et al., 2018, 2019).

5.9. Validation protocols

The reviewed literature indicates that most wearable robots were validated through walking experiments conducted either on level ground or on a treadmill. However, a significant limitation of these validation experiments was the small number of participants. Over 40% of the studies relied on data from just a single subject, which raises concerns about the representativeness and generalizability of the findings. Results derived from a single individual may be biased by their unique characteristics and are unlikely to achieve statistical significance. To draw robust conclusions, validation studies should ideally include a larger and more diverse participant pool.

The evaluation of control strategies in these studies predominantly focused on gait kinematics and kinetics. Key metrics assessed included: (i) angular positions and velocities (Ahmed et al., 2017; Akbari et al., 2023; Akkawutvanich & Manoonpong, 2023; Eken et al., 2023; Fang et al., 2014; Gui et al., 2017a, 2017b; Huang et al., 2018, 2019; Hwang et al., 2021; Luo et al., 2022; Mehr et al., 2023, 2021; Plaza et al., 2022; Qiu et al., 2020, 2021; Ren & Zhang, 2014; Sharifi et al., 2021, 2022; Wang et al., 2019; Xu et al., 2022; Yuan et al., 2019; Zhang et al., 2018, 2017; Zhang & Zhang, 2022; Zou et al., 2020); (ii) interaction forces/torques (Huang et al., 2019; Mehr et al., 2023; Plaza et al., 2022; Ren & Zhang, 2014; Sharifi et al., 2022; Wang et al., 2019; Zhang et al., 2018, 2017); (iii) ground reaction forces (Chen et al., 2017; Wang et al., 2022); (iv) muscle activity measured via EMG signals (Qiu et al., 2020; Tsukahara et al., 2017); and (v) metabolic cost measurements (Tsukahara et al., 2017). Additionally, some studies gathered subjective feedback from participants, capturing their perceptions of the exoskeleton's performance and comfort (Yuan et al., 2019).

Most studies primarily evaluated the controllers' performance based on their ability to track the desired trajectory, using metrics such as maximum error, MAE, nMSE, and RMSE. In addition to trajectory tracking accuracy, a few studies also considered other performance indicators, including convergence time and controller processing or actuation delay. However, these metrics were rarely reported, each appearing only once in the reviewed literature (Akkawutvanich & Manoonpong, 2023; Gui et al., 2017b).

Many studies conducted inadequate evaluations, relying solely on comparisons between the expected and actual outputs without providing explicit quantitative indices. This lack of detailed reporting makes it difficult to establish a global benchmarking system. Benchmarking, which involves comparing a system's performance against standardized metrics, is crucial for wearable robotics (Torricelli et al., 2020). To address this, the academic community is increasingly advocating for standardized controller validation. This would enhance transparency in comparing bio-inspired approaches while keeping user needs central to wearable robotics development.

5.10. Outcomes

The vast majority aimed to assess whether CPG- and DMP-based controllers could generate stable gait patterns and enable smooth modulation to address different locomotion challenges.

Overall, findings consistently demonstrated that these bio-inspired approaches exhibit a remarkable ability to produce stable movement patterns while allowing seamless modulation in amplitude, frequency, and phase. This adaptability ensures that the requirements of the locomotive in terms of safety, balance, adaptation to the environment and adaptation to the individual characteristics of its users are met.

In studies that evaluated tracking performance during human trials, results indicated that the devices accurately followed the generated gait patterns, typically resulting in trajectories tracking errors below 6 ° (Ahmed et al., 2017; Mehr et al., 2023, 2021; Ren & Zhang, 2014; Sharifi et al., 2021, 2022; Xu et al., 2022; Yingxu et al., 2019).

Beyond trajectory tracking, a smaller subset of studies examined the direct impact of the bio-inspired controllers on human biomechanics. These investigations concluded that control strategies improved

the smoothness of patients' gait compared to the unassisted condition (Tsukahara et al., 2017), reduced upper limb exertion when using a device with crutches (Chen et al., 2017; Wang et al., 2022), and minimized interaction forces between the user and the device compared to the Sensitivity Amplification Control (SAC) (Wang et al., 2019). Additionally, reductions in muscular effort and metabolic cost were observed when walking with a wearable device, both in comparison to walking without assistance and with the device operating in transparent mode (Qiu et al., 2021).

More information about the results and conclusions for each article included in the review can be found in [Appendix B](#).

5.11. Challenges and limitations

The implementation of CPGs and DMPs remains a challenging task, as both approaches require careful parametrization and tuning. Their performance depends on the accurate selection and initialization of parameters. As controller complexity increases – particularly with higher dimensionality – these systems become less computationally efficient and more sensitive to environmental changes and disturbances (Akkawutvanich & Manoonpong, 2023). Achieving optimal control stability and precision demands meticulous optimization of parameters and gains (Mehr et al., 2023).

Regarding CPG tuning, most studies relied on manual adjustment methods (Ahmed et al., 2017; Akbari et al., 2023; Gui et al., 2015; Luo et al., 2018; Sharifi et al., 2022; Yingxu et al., 2019; Zhang et al., 2018, 2017). However, some employed optimization algorithms, such as Genetic Algorithms (GA) (Fang et al., 2014; Gui et al., 2017b; Schrade et al., 2017; Wang et al., 2022) or Harmony Search Algorithm (HSA) (Mokhtari et al., 2022) to identify optimal parameters. Given the number of parameters involved, one study adopted a hybrid approach, selectively optimizing only certain parameters to streamline the process (Schrade et al., 2017). For DMP learning, the majority of the reviewed articles used regression models (Huang et al., 2018, 2019; Hwang et al., 2021; Luo et al., 2022; Ma et al., 2020; Qiu et al., 2020; Wang & Wang, 2020; Xu et al., 2022) and RL approaches (Chen et al., 2017; Huang et al., 2020; Wang et al., 2019; Yuan et al., 2019; Zhang & Zhang, 2022).

A persistent challenge in this field is the need for online parameter tuning to accommodate the unique requirements of individual users when walking with an exoskeleton. Machine Learning (ML) techniques show potential in addressing this issue, enabling personalized and adaptive assistance. However, factors like variations in walking behaviour and convergence times across individuals continue to make truly personalized assistance difficult to achieve (Akbari et al., 2023).

Another limitation lies in the limited integration of user authority within control systems. The adjustment process often lags behind real-time changes in human movement intentions, leading to energy losses and reduced adaptability. To address this, control algorithms need to predict user intentions rather than merely react to them (Ahmed et al., 2017). One promising approach is the Frequency Adaptive DMP (FADMP) (Qiu et al., 2021), which provides predictive control and rapid convergence to input signals. However, FADMP is limited to scenarios where walking frequency remains stable, which fails to capture the variability of real-world conditions.

In CPG-based control, system performance is closely linked to the architecture's topology. Designing effective topologies for specific tasks remains a complex and non-trivial process, and these designs often lack adaptability to different scenarios.

Furthermore, safety is another critical consideration in developing CPG- and DMP-based control systems. Embedding robust safety mechanisms within the control architecture is essential to protect users in all operating conditions (Schrade et al., 2017). Unfortunately, many studies failed to incorporate adequate safety measures, raising concerns. These systems rely on online feedback signals that can be corrupted

by noise or perturbed by internal and external disturbances. Stability must be guaranteed under all conditions to ensure safe operation.

Finally, another challenge lies in balancing system control with user control. Effective control strategies must allow the user to retain authority while ensuring that the system operates safely and reliably. Striking this balance is essential for achieving practical and user-friendly solutions in wearable robotics.

6. Conclusion

This narrative review has outlined the current advancements in two bio-inspired control methods – Central Pattern Generators (CPGs) and Dynamic Movement Primitives (DMPs) – and their application in lower limb exoskeletons and orthoses. Since 2011, research in bio-inspired control for wearable robotic systems has gained significant interest, driven by the advantages they offer in improving user-device interaction. CPGs and DMPs enhance wearable robotics by enabling adaptive, stable movement, ensuring precise trajectory tracking, and facilitating smooth transitions across various locomotion conditions.

In summary, CPG architectures, while complex, integrate various types of oscillating units to generate control signals for joint angular position, torque, and stiffness. DMPs, available in both discrete and periodic formulations, can similarly produce joint position and torque in both joint and task spaces, depending on the specific control objectives. These methods have been implemented for different purposes, including trajectory planning and movement generation, and they leverage feedback from a range of sensors for real-time modulation. This feedback enables on-the-fly adjustments to trajectories, supporting adaptability to disturbances, personalization and improving user autonomy.

Despite their benefits, further research is needed to overcome some of their limitations. The complexity of the mathematical models, the difficulty in timely and accurate intention decoding, and the lack of stability and safety measures in many studies hinder progress. Additionally, the methods reviewed employ different performance metrics – such as trajectory tracking accuracy, adaptability to disturbances, and computational efficiency – making direct quantitative comparisons challenging. Furthermore, inconsistencies in evaluation protocols reduce the ability to make rigorous cross-study comparisons.

Nevertheless, bio-inspired control methods have demonstrated their versatility in managing multi-degree-of-freedom robotic systems. Future research should continue exploring these techniques to unlock their full potential, particularly in improving safety, adaptability, and real-time user interaction.

Declaration of competing interest

The authors declare that they have no known competing financial interests or personal relationships that could have appeared to influence the work reported in this paper.

Appendix A. Mathematical formulations

A.1. CPGs equations

Phase Oscillator

This oscillator was mentioned in most of the articles and presented several variations to its equations. The three articles by Gui et al. (2015) refer to this oscillator as a Sine CPG. The generic equations that describe its behaviour are:

$$\dot{\phi}_i(t) = \omega_i + \sum_{j=1}^N v_{ij} \sin(\phi_j(t) - \phi_i(t) - \Phi) \quad (A.1)$$

$$\ddot{x}_i(t) = \mu \left[\frac{\mu}{4} (X_i - x_i(t)) - \dot{x}_i(t) \right] \quad (A.2)$$

Table B.4

Results and conclusions of the articles implementing CPG/DMP control strategies (SIM - Simulation; HE - Human Experiments).

Article	Objective	Method	Results	Conclusions
Duvinage et al. (2011)	Tests two phase resetting mechanism	SIM	The hard phase-resetting converges quickly and recovers faster than the soft phase reset	PCPG allows for easy modulation of amplitude and frequency to adapt to gait phases
Fang et al. (2014)	Verify gait patterns at two different frequencies and the transitions	HE	CPG achieved a smooth transition between the two states	This method is valid for paraplegic rehabilitation
Ren and Zhang (2014)	Validate CPG performance for control of a hybrid (FES + Exo) system	HE	CPG ensured that the FES trajectory remained in sync with the actual joint angle without delay	The method is useful to create the trajectories for both assistance types and maintain synchrony
Ajai et al. (2015)	Validate CPG performance for gait pattern generation	SIM	Minimal tracking error (<0.02°) while keeping torque within safe limits	CPG has good tracking performance and stability, ensuring user safety
Gui et al. (2015)	Assess BCI performance and CPG adaptation to higher level orders	HE	BCI: DOT of 1.69% and ROS of 92.40%, and CPG generated adequate movement patterns	The exoskeleton achieved smooth movement due to CPG's properties
Gui et al. (2017a)	Evaluate CPG performance in response to voluntary EMG of subjects	HE	CPG adjusted frequency and amplitude to muscle contractions controlling the knee joint	CPG produced stable and coordinated movement in response to pHRI
Gui et al. (2017b)	Evaluate CPG performance in response to both pHRI and cHRI modulation	HE	BCI was able to detect all locomotion modes and pHRI adjusted the frequency of movement	CPG produced stable and coordinated movement in response to pHRI and cHRI
Schrade et al. (2017)	Evaluate CPG adaptability to produce gait in different environments	SIM	CPG produced stable gait patterns on flat ground (0.4 to 1.57 m/s), downward slopes (up to 15°), and upward slopes (up to 3°)	CPG control is well suited for bipedal locomotion of an exoskeleton model when a torso stabilizing torque is present.
Zhang et al. (2017)	Validate CPG behaviour for generating coordinated motion with different frequencies and amplitudes	HE	The trajectory tracking was smooth and stable, even during transitions, and achieved maximum errors of 3°	The control method provides an effective solution for dealing with the coordination between FES and the exoskeleton in a hybrid system.
Tsukahara et al. (2017)	Verify the effectiveness of the wearable system controlled using a CPG for patients with SCD	HE	The Harmonic Ratio of the patients in the vertical direction increased with statistical significance	The smoothness of the patients' gait improved when walking with the system
Ahmed et al. (2017)	Verify the intention detection using HCT and the adjustment of the CPG frequency	SIM	The tracking error of less than 3° when transit from 0.5 to 1 m/s	The pilot's intentions were estimated and the walking speed was adjusted with acceptable performance
Chen et al. (2017)	Verify the convergence of the algorithm for finding optimal step length and analyse the effects on the user	SIM/HE	DMP is able to reduce trunk torque and the pressure applied by the user to walk with the device and crutches	The method presents better performance compared to other fixed methods, being able to reduce the person's effort, while maintaining stability
Zhang et al. (2018)	Validate if the proposed control method is able to generate adequate gait patterns	SIM/HE	CPG generates stable gait pattern and can change from autonomous to synchronous oscillation	CPG networks allow adequate HRI to be achieved and improves the flexibility with respect to master/slave motion
Luo et al. (2018)	Evaluate CPG control patterns and interaction with a human model	SIM	CPG output is smooth and tracking performance is proper	The simulation results show that the proposed method has great potential in controlling assistive exoskeleton in a more biological way
Chen et al. (2018)	Evaluate DMP ability to maintain stability under different disturbances	SIM	The gait generated using DMP achieves balance with external forces up to 15N	The step planner is efficient in counteracting external disturbances
Huang et al. (2018)	Analyse DMP learning method and verify adequacy of gait patterns for different velocities	SIM/HE	The proposal achieves less nMSE than traditional SAC (0.026 compared to 0.076 rad)	Experimental results show that the proposed HIL control strategy is able to deal with varying interaction dynamics
Yingxu et al. (2019)	Check whether CPG can generate different types of motion curves	SIM/HE	Hip and knee with average error of 5.2° and 2.1° and average lag time of 0.83s and 0.64s, respectively	CPG neural network model can meet the control needs of exoskeleton
Yuan et al. (2019)	Analyse DMP-RL approach in learning joint trajectories while eliminating disturbances	HE	RL can suppress uncertainties and DMP generates adequate walking patterns	The method allows for the trajectories to be constantly adjusted and smoothly trace the target pattern
Huang et al. (2019)	Evaluate CCP performance for different walking conditions and subjects	SIM/HE	The algorithm can make the device follow the pilot's motion with little tracking error in transition cycle, indicating a reduction of pHRI	CCP are able to model and learn the pilot's motion trajectories online through pHRI between the pilot and the exoskeleton

(continued on next page)

Table B.4 (continued).

Article	Objective	Method	Results	Conclusions
Wang et al. (2019)	Validate DMP learning method and illustrate the control performance in comparison to SAC	HE	The algorithm presented better performance both in convergence and learning speed and the control achieved reduced HMI compared to SAC	The results showed promising control learning and performance, while ensuring stable locomotion
Chen et al. (2020a)	Evaluate CPG reliability for locomotion	SIM/HE	The activity of each neuron converged to a steady state	The method generated steady walking motion
Chen et al. (2020b)	Evaluate CPG reliability for locomotion	SIM/HE	CPG control commands indicate that it can generate stable and human-like patterns	CPG control model could converge to a steady state
Huang et al. (2020)	Validate DMP behaviour for movement generation during inclined walking	SIM/HE	DMP dynamically adjusted foot locations, reducing tracking error in sequential steps	The approach provided the exoskeleton with the ability to walk dynamically on slopes with different gradients
Ma et al. (2020)	Verify the adaptability of DMP to generate walking patterns for a range of velocities	SIM	The produced trajectories were modified both in frequency and amplitude for velocities ranging from 0.5 to 1.5 m/s, similar to human behaviour	The imitation system has the strong ability to replicate demonstration trajectories and output anthropomorphic gait at different speeds
Qiu et al. (2020)	Validate DMP for learning personalized patterns and predict stable trajectories	HE	DMP reproduced a stable and adapted trajectory with a delay of less than 10ms and a small AME (< 4°)	DMP model allowed to predict smooth and personalized motion patterns during walking with reduced noise and delay
Wang and Wang (2020)	Evaluate the learning process of DMPs using three distinct algorithms	SIM	GRNN-DMP achieved the smallest tracking error (<0.003°) indicating a stronger fitting ability	The proposed method is verified to have the better learning ability and larger leaning rate towards expected joint trajectory
Zou et al. (2020)	Validate the algorithm for slope gradient detection and DMP adaptability for slopes	HE	The method adequately estimated slope gradients and foot locations are dynamically adjusted to reduce the tracking error	Experimental results indicate that the proposed approach endows the exoskeleton with the ability to walk dynamically on slopes with different gradients
Sharifi et al. (2021)	Evaluate CPG modulation according to the imposed torques of the user	HE	Suitable tracking performance with errors of 2° and 0° for the hip and knee, respectively	This adaptiveness was facilitated by the amendment of the gait frequency, amplitudes, and equilibrium position of reference trajectories
Mehr et al. (2021)	Analyse hip adjustment and the effect of HRI in the CPGs modulation	HE	The maximum errors of the hip and the knee of 0.6° and 1.1°, respectively	The strategy proved its effectiveness in proving postural stability and adaptation of motion
Xu et al. (2021)	Validate DMP with balance control strategy feasibility to walk continually without falling	SIM/HE	All planned gaits are well-executed, with errors meeting the requirements and with the ability to adjust gait features based on stability detection	The gait generator could tune different gaits to keep the system safe according to the spatial and temporal features of DMPs
Qiu et al. (2021)	Validate FADMPs performance with different parameters and evaluate the control effect on human users compared to Fre, OFF and TRA conditions	SIM/HE	The device does not restrict human motion during assistance, the muscle activity is reduced compared to OFF and TRA conditions and reduces metabolic power	The experiment results show that the proposed control framework can improve the RoM, reduce muscle activity and cut down the metabolic cost
Hwang et al. (2021)	Verify DMP ability to adjust gait parameters based on human intention	SIM/HE	The results indicate that through a single parameter is it possible to adjust step length for appropriate user adaptation	The method can be useful for ADLs with various stride lengths and ensure patient safety while walking
Wang et al. (2022)	Validate that the strategy is able to reduce the user's effort for load carrying	SIM/HE	The decrement ratio of vGRF with wearing the exoskeleton is 66.6% and 55.4%, respectively	This method makes the exoskeleton reduce the human body's sense of weight bearing
Mokhtari et al. (2022)	Examine CPG robustness in the presence of disturbances compared to other methods	SIM	The tracking error of the CPG controller was lower than 0.3° and interaction forces were reduced	The proposed CPG controller resulted in increased robustness, decreased interaction forces, and alleviated chattering compared to conventional methods
Sharifi et al. (2022)	Evaluate DO performance in detecting human intentions and CPG modulation	HE	Appropriate tracking performance with errors of less than 1° and smooth adjustment of frequency, amplitude and phase	The autonomous control scheme facilitated flexible and personalized locomotion based on HRI for lower-limb exoskeleton
Plaza et al. (2022)	Analyse CPG performance in controlling different exoskeleton configurations and generating various patterns	HE	CPG provided the expected synchronized movement and managed to maintain stability during frequency and amplitude changes	The control method can maintain coordination and communication among the joints of the network in all proposed configurations

(continued on next page)

Table B.4 (continued).

Article	Objective	Method	Results	Conclusions
Xu et al. (2022)	Evaluate DMP with DCM for planning footsteps during walking	HE	The method achieves smooth walking devoid of significant disturbance and with tracking error confined to 6°	The algorithm allowed the exoskeleton robot's trajectories to be continuously adjusted, and the goal trajectory could be tracked smoothly
Zhang and Zhang (2022)	Evaluate DMP-RL approach for learning new motion patterns online	HE	The method is able to suppress uncertainty and interference, demonstrating effectiveness to assist human motion for stable walking	Combining DMPs with RL allowed to continuously adjusted the robot's motion to track the target trajectory smoothly
Tan et al. (2022)	Analyse DMP performance with CBF for improving flexibility and safety	SIM	The simulation result retains the original walking trajectory and it meets the requirements of the safety set	DMP proved important for trajectory adjustment in rehabilitation and the introduction of CBF ensured the safety of the wearer
Luo et al. (2022)	Evaluate the dynamic online adjustment of reference trajectories through DMP and path-based control	SIM/HE	The method present reduces tracking error compared to others and improved user's freedom to control leg movement	The results showed that the control strategy is able to adapt to gait features, enhance subjects' gait performance, and allow the subjects to change the gait pattern
Wang et al. (2024)	Validate CPG controller's ability to track the interaction torque	SIM	ACPG adjusts both frequency and amplitude in accordance with the active torque of the user (Error<3°)	The rehabilitation gait can be adjusted online according to the patient's lower limb muscle strength level
Mehr et al. (2023)	Evaluate Deep RL performance for facilitating the user to reach the desired trajectory	SIM/HE	The user could change the iCPG frequency on average in 10s with max errors of 6° and 4° for the knee and hip	The results showed that the method could be used for personalized motion planning
Akkawutvanich and Manoonpong (2023)	Verify the controller performance for human adaptation, for walking in various conditions and for improved coordination	HE	CPG converges to the user's walking frequency and presented good tracking (MAE<5°) for different walking speeds and conditions	CPG can adapt to the different walking styles of five subjects with a total average time less than 2 min and can handle dynamic environments
Akbari et al. (2023)	Evaluate the effect of incorporating Uncertainty Analysis into a CPG for detecting unsafe operations	HE	The algorithm cancels the effect of unsafe action in the trajectory generated by CPG that is smoothly adjusted	The proposed technique was able to detect unsafe decisions of the exoskeleton and tuned CPGs gains considering the level of uncertainty
Eken et al. (2023)	Evaluate DMP method for continuous phase estimation during different locomotion modes compared to other methods	HE	The tests revealed that an aDMP model could estimate the gait phase on average with $3.98 \pm 1.33\%$ RMSE and $0.60 \pm 0.55\%$ error at the step offset	aDMP for phase estimation demonstrated a similar and even superior performance for some locomotion modes compared to other algorithms

The variable x can denote different properties of the oscillator, i.e. frequency f , amplitude α and equilibrium position ξ , according to the approaches included in the review. The output of each oscillator described by the above equations can have different formulations, usually composed of sine and/or cosine functions. Examples of those are:

$$y_i(t) = \alpha_i(t) \sin(\phi_i(t)) \quad (\text{A.3})$$

$$y_i(t) = \alpha_i(t) \cos(\phi_i(t)) \quad (\text{A.4})$$

$$y_i(t) = \xi_i(t) + \alpha_i(t) \sum_{l=1}^{S_i} (c_{il} \cos(l\phi_i(t)) + d_{il} \sin(l\phi_i(t))) \quad (\text{A.5})$$

Matsuoka Oscillator

The oscillation dynamics of each neuron can be represented by:

$$T_r \dot{x}_i(t) + x_i(t) = - \sum_{j=1}^N w_{ij} y_j(t) + s_i + e_i(t) - b r_i(t) \quad (\text{A.6})$$

$$T_a \dot{r}_i(t) + r_i(t) = y_i(t) \quad (\text{A.7})$$

$$y_i(t) = \max \{0, x_i(t)\} \quad (\text{A.8})$$

where T_a and T_r are time constants; $x_i(t)$ denotes the neuron's potential; w_{ij} denotes the weight of the inhibitory effect from the j th neuron to the i th neuron; $e_i(t)$ represents the sensory feedback; $r_i(t)$ is the adaptation rate; b is a constant of the steady-state firing rate; and $y_i(t)$ denotes the output of the i th neuron.

Hopf Oscillator

The Hopf oscillator can be described by the following ordinary differential equations:

$$\dot{x} = (\mu^2 - (x^2 + y^2))x + \omega y \quad (\text{A.9})$$

$$\dot{y} = (\mu^2 - (x^2 + y^2))y + \omega x \quad (\text{A.10})$$

where x, y are the states of the oscillator, ω is the intrinsic frequency and μ determines the steady-state amplitude of the oscillation.

In order to provide the oscillators with the capability of self-tuning to the frequency components of the input signal autonomously, a formulation of Hopf oscillators with frequency adaptation was later proposed. The equations comprising this change are as follows,

$$\dot{x}_i = \gamma(\mu^2 - r_i^2)x_i + \omega_i y_i + \epsilon F(t) + \tau \sin(R_i - \varphi_i) \quad (\text{A.11})$$

$$\dot{y}_i = \gamma(\mu^2 - r_i^2)y_i + \omega_i x_i \quad (\text{A.12})$$

$$\dot{\omega}_i = -\epsilon F(t) \frac{y_i}{r_i} \quad (\text{A.13})$$

$$\dot{\alpha}_i = \eta x_i F(t) \quad (\text{A.14})$$

$$\dot{\phi}_0 = 0 \quad (\text{A.15})$$

$$\dot{\phi}_i = \sin(R_i - \text{sgn}(x_i) \cos^{-1}(-\frac{y_i}{r_i})) - \phi_i \quad (\text{A.16})$$

$$R_i = \frac{\omega_i}{\omega_0} \text{sgn}(x_0) \cos^{-1}(-\frac{y_i}{r_0}) \quad (\text{A.17})$$

where ϵ is a coupling constant and $F(t)$ is the input.

Van der Pol's Oscillator

The differential equation that governs this oscillator is given by Eq. (A.18), where $i = 1, \dots, N$, N as the number of units, $x_i(t)$ denotes

the output signal, p_i^2 represents the amplitude, g_i^2 is the frequency, ϕ_i denotes the offset parameter, μ_i indicates the nonlinearity and the damping strength while $x_k(t)$ are the coupling equations defined depending on the coupling methodology employed.

$$\ddot{x}_i(t) - \mu_i(p_i^2 - x_k^2)\dot{x}_i(t) + g_i^2x_k(t) = \phi_i \quad (\text{A.18})$$

A.2. Periodic DMPs

The rhythmic variant of DMPs is defined by Eqs. (A.19) to Eq. (A.21). The main difference from the discrete formulation is the replacement of the temporal parameter, τ , with the system's frequency, Ω . Another modification lies in the phase variable, denoted as ϕ , which is governed by a dynamical system that controls the progression of each motion cycle. Eq. (A.21) represents a linear phase progression, but alternative approaches can also be used to define this variable.

$$\dot{z} = \Omega\alpha(\beta(g - y) - z) + f(\phi) \quad (\text{A.19})$$

$$\dot{y} = \Omega z \quad (\text{A.20})$$

$$\dot{\phi} = \Omega \quad (\text{A.21})$$

Appendix B. Summary of results and conclusions per article

See Table B.4.

Data availability

No data was used for the research described in the article.

References

- Acebrón, J. A., Bonilla, L. L., Vicente, C. J. P., Ritort, F., & Spigler, R. (2005). The kuramoto model: A simple paradigm for synchronization phenomena. *Reviews of Modern Physics*, 77(1), 137.
- Ahmed, A. I., Cheng, H., Lin, X., Elhassan, Z. M., & Omer, M. (2017). On-line walking speed control in human-powered exoskeleton systems. In *2017 international conference on communication, control, computing and electronics engineering* (pp. 1–7). IEEE.
- Ajayi, M. O., Djouani, K., & Hamam, Y. (2015). Bounded control of a full-exoskeleton device with four (4) degree of freedom. In *2015 IEEE international conference on robotics and biomimetics* (pp. 2425–2430). IEEE.
- Akbari, M., Mehr, J. K., Ma, L., & Tavakoli, M. (2023). Uncertainty-aware safe adaptable motion planning of lower-limb exoskeletons using random forest regression. *Mechatronics*, 95, Article 103060.
- Akkawutvanich, C., & Manoonpong, P. (2023). Personalized symmetrical and asymmetrical gait generation of a lower-limb exoskeleton. *IEEE Transactions on Industrial Informatics*.
- Baud, R., Manzoori, A. R., Ijspeert, A., & Bouri, M. (2021). Review of control strategies for lower-limb exoskeletons to assist gait. *Journal of NeuroEngineering and Rehabilitation*, 18(1), 1–34.
- Chen, Q., Cheng, H., Yue, C., Huang, R., & Guo, H. (2017). Step length adaptation for walking assistance. In *2017 IEEE international conference on mechatronics and automation* (pp. 644–650). IEEE.
- Chen, Q., Cheng, H., Yue, C., Huang, R., Guo, H., et al. (2018). Dynamic balance gait for walking assistance exoskeleton. *Applied Bionics and Biomechanics*, 2018.
- Chen, W., Wang, J., Zhang, J., Chen, W., Zhao, Z., et al. (2020a). Bio-inspired control of lower limb exoskeleton using a central pattern generator. In *2020 Chinese control and decision conference* (pp. 2041–2046). IEEE.
- Chen, W., Wang, J., Zhang, J., Chen, W., Zhao, Z., et al. (2020b). Adaptive locomotion of lower limb exoskeleton based on oscillators and frequency adaptation. In *2020 15th IEEE conference on industrial electronics and applications* (pp. 1550–1555). IEEE.
- Duvinage, M., Jiménez-Fabián, R., Castermans, T., Verlinden, O., & Dutoit, T. (2011). An active foot lifter orthosis based on a pcpg algorithm. In *2011 IEEE international conference on rehabilitation robotics* (pp. 1–7). IEEE.
- Eken, H., Pergolini, A., Mazzarini, A., Livolsi, C., Fagioli, I., Penna, M. F., et al. (2023). Continuous phase estimation in a variety of locomotion modes using adaptive dynamic movement primitives. In *2023 international conference on rehabilitation robotics* (pp. 1–6). IEEE.
- Fang, J., Ren, Y., & Zhang, D. (2014). A robotic exoskeleton for lower limb rehabilitation controlled by central pattern generator. In *2014 IEEE international conference on robotics and biomimetics* (pp. 814–818). IEEE.
- Gantenbein, J., Dittli, J., Meyer, J. T., Gassert, R., & Lamberty, O. (2022). Intention detection strategies for robotic upper-limb orthoses: a scoping review considering usability, daily life application, and user evaluation. *Frontiers in Neurorobotics*, 16, Article 815693.
- Grosse-Wentrup, M., Mattia, D., & Oweiss, K. (2011). Using brain–computer interfaces to induce neural plasticity and restore function. *Journal of Neural Engineering*, 8(2), Article 025004.
- Gui, K., Liu, H., & Zhang, D. (2017a). A generalized framework to achieve coordinated admittance control for multi-joint lower limb robotic exoskeleton. In *2017 international conference on rehabilitation robotics* (pp. 228–233). IEEE.
- Gui, K., Liu, H., & Zhang, D. (2017b). Toward multimodal human–robot interaction to enhance active participation of users in gait rehabilitation. *IEEE Transactions on Neural Systems and Rehabilitation Engineering*, 25(11), 2054–2066.
- Gui, K., Ren, Y., & Zhang, D. (2015). Online brain–computer interface controlling robotic exoskeleton for gait rehabilitation. In *2015 IEEE international conference on rehabilitation robotics* (pp. 931–936). IEEE.
- Huang, R., Cheng, H., Guo, H., Lin, X., & Zhang, J. (2018). Hierarchical learning control with physical human-exoskeleton interaction. *Information Sciences*, 432, 584–595.
- Huang, R., Cheng, H., Qiu, J., & Zhang, J. (2019). Learning physical human–robot interaction with coupled cooperative primitives for a lower exoskeleton. *IEEE Transactions on Automation Science and Engineering*, 16(4), 1566–1574.
- Huang, R., Wu, Q., Qiu, J., Cheng, H., Chen, Q., & Peng, Z. (2020). Adaptive gait planning with dynamic movement primitives for walking assistance lower exoskeleton in uphill slopes. *Sensors & Materials*, 32.
- Hwang, S. H., Sun, D. I., Han, J., & Kim, W.-S. (2021). Gait pattern generation algorithm for lower-extremity rehabilitation–exoskeleton robot considering wearer's condition. *Intelligent Service Robotics*, 14, 345–355.
- Ijspeert, A. J. (2008). Central pattern generators for locomotion control in animals and robots: a review. *Neural Networks*, 21(4), 642–653.
- Ijspeert, A. J., Nakanishi, J., Hoffmann, H., Pastor, P., & Schaal, S. (2013). Dynamical movement primitives: learning attractor models for motor behaviors. *Neural Computation*, 25(2), 328–373.
- Ijspeert, A. J., Nakanishi, J., & Schaal, S. (2002a). Movement imitation with nonlinear dynamical systems in humanoid robots. In *Proceedings 2002 IEEE international conference on robotics and automation (cat. no. 02CH37292)*: vol. 2, (pp. 1398–1403). IEEE.
- Ijspeert, A. J., Nakanishi, J., & Schaal, S. (2002b). Learning rhythmic movements by demonstration using nonlinear oscillators. In *Proceedings of the IEEE/RSJ international conference on intelligent robots and systems* (pp. 958–963).
- Luo, L., Foo, M. J., Ramanathan, M., Er, J. K., Chiam, C. H., Li, L., et al. (2022). Trajectory generation and control of a lower limb exoskeleton for gait assistance. *Journal of Intelligent and Robotic Systems*, 106(3), 64.
- Luo, R., Sun, S., Zhao, X., Zhang, Y., & Tang, Y. (2018). Adaptive cpg-based impedance control for assistive lower limb exoskeleton. In *2018 IEEE international conference on robotics and biomimetics* (pp. 685–690). IEEE.
- Ma, W., Huang, R., Chen, Q., Song, G., & Li, C. (2020). Dynamic movement primitives based parametric gait model for lower limb exoskeleton. In *2020 39th Chinese control conference* (pp. 3857–3862). IEEE.
- Matos, V., & Santos, C. P. (2014). Towards goal-directed biped locomotion: Combining cpes and motion primitives. *Robotics and Autonomous Systems*, 62(12), 1669–1690.
- Matsuoka, K. (1985). Sustained oscillations generated by mutually inhibiting neurons with adaptation. *Biological Cybernetics*, 52(6), 367–376.
- Mehr, J. K., Guo, E., Akbari, M., Mushahwar, V. K., & Tavakoli, M. (2023). Deep reinforcement learning based personalized locomotion planning for lower-limb exoskeletons. In *2023 IEEE international conference on robotics and automation* (pp. 5127–5133). IEEE.
- Mehr, J. K., Sharifi, M., Mushahwar, V. K., & Tavakoli, M. (2021). Intelligent locomotion planning with enhanced postural stability for lower-limb exoskeletons. *IEEE Robotics and Automation Letters*, 6(4), 7588–7595.
- Mokhtari, M., Taghizadeh, M., & Ghaf-Ghanbari, P. (2022). Adaptive second-order sliding model-based fault-tolerant control of a lower-limb exoskeleton subject to tracking the desired trajectories augmented by cpg algorithm. *Journal of the Brazilian Society of Mechanical Sciences and Engineering*, 44(9), 423.
- Niazi, I. K., Jiang, N., Tiberghien, O., Nielsen, J. F., Dremstrup, K., & Farina, D. (2011). Detection of movement intention from single-trial movement-related cortical potentials. *Journal of Neural Engineering*, 8(6), Article 066009.
- Plaza, A., Hernandez, M., Gutierrez, A., Ramos, J., Puyuelo, G., Cumplido, C., et al. (2022). Design of a modular exoskeleton based on distributed central pattern generators. *IEEE Systems Journal*, 17(1), 816–827.
- Qiu, S., Guo, W., Caldwell, D., & Chen, F. (2020). Exoskeleton online learning and estimation of human walking intention based on dynamical movement primitives. *IEEE Transactions on Cognitive and Developmental Systems*, 13(1), 67–79.
- Qiu, S., Guo, W., Zha, F., Deng, J., & Wang, X. (2021). Exoskeleton active walking assistance control framework based on frequency adaptive dynamics movement primitives. *Frontiers in Neurorobotics*, 15, Article 672582.
- Qiu, S., Pei, Z., Wang, C., & Tang, Z. (2023). Systematic review on wearable lower extremity robotic exoskeletons for assisted locomotion. *Journal of Bionic Engineering*, 20(2), 436–469.

- Ren, Y., & Zhang, D. (2014). Fexo knee: A rehabilitation device for knee joint combining functional electrical stimulation with a compliant exoskeleton. In *5th IEEE RAS/EMBS international conference on biomedical robotics and biomechatronics* (pp. 683–688). IEEE.
- Righetti, L., & Ijspeert, A. J. (2006). Programmable central pattern generators: an application to biped locomotion control. In *Proceedings 2006 IEEE international conference on robotics and automation, 2006* (pp. 1585–1590). IEEE.
- Santos, C. P., Alves, N., & Moreno, J. C. (2017). Biped locomotion control through a biomimetic cpg-based controller. *Journal of Intelligent and Robotic Systems*, 85, 47–70.
- Saveriano, M., Abu-Dakka, F. J., Kramberger, A., & Peternel, L. (2023). Dynamic movement primitives in robotics: A tutorial survey. *The International Journal of Robotics Research*, 42(13), 1133–1184.
- Schaal, S. (2006). Dynamic movement primitives-a framework for motor control in humans and humanoid robotics. In *Adaptive motion of animals and machines* (pp. 261–280). Springer.
- Schrade, S. O., Nager, Y., Wu, A. R., Gassert, R., & Ijspeert, A. (2017). Bio-inspired control of joint torque and knee stiffness in a robotic lower limb exoskeleton using a central pattern generator. In *2017 international conference on rehabilitation robotics* (pp. 1387–1394). IEEE.
- Sharifi, M., Mehr, J. K., Mushahwar, V. K., & Tavakoli, M. (2021). Adaptive cpg-based gait planning with learning-based torque estimation and control for exoskeletons. *IEEE Robotics and Automation Letters*, 6(4), 8261–8268.
- Sharifi, M., Mehr, J. K., Mushahwar, V. K., & Tavakoli, M. (2022). Autonomous locomotion trajectory shaping and nonlinear control for lower limb exoskeletons. *Ieee/ASME Transactions on Mechatronics*, 27(2), 645–655.
- Sun, Y., Tang, Y., Zheng, J., Dong, D., Chen, X., & Bai, L. (2022). From sensing to control of lower limb exoskeleton: A systematic review. *Annual Reviews in Control*, 53, 83–96.
- Tan, D.-P., Cao, G.-Z., Zhang, Y.-P., Chen, J.-C., & Li, L.-L. (2022). Safe movement planning with dmp and cbf for lower limb rehabilitation exoskeleton. In *2022 19th international conference on ubiquitous robots* (pp. 231–236). IEEE.
- Torricelli, D., Rodriguez-Guerrero, C., Veneman, J. F., Crea, S., Briem, K., Lenggenhager, B., et al. (2020). Benchmarking wearable robots: challenges and recommendations from functional, user experience, and methodological perspectives. *Frontiers in Robotics and AI*, 7, Article 561774.
- Tsukahara, A., Yoshida, K., Matsushima, A., Ajima, K., Kuroda, C., Mizukami, N., et al. (2017). Evaluation of walking smoothness using wearable robotic system curara® for spinocerebellar degeneration patients. In *2017 international conference on rehabilitation robotics* (pp. 1494–1499). IEEE.
- Tucker, M. R., Olivier, J., Pagel, A., Bleuler, H., Bouri, M., Lambery, O., et al. (2015). Control strategies for active lower extremity prosthetics and orthotics: a review. *Journal of Neuroengineering and Rehabilitation*, 12(1), 1–30.
- Wang, L., Chen, C., Dong, W., Du, Z., Shen, Y., & Zhao, G. (2019). Locomotion stability analysis of lower extremity augmentation device. *Journal of Bionic Engineering*, 16, 99–114.
- Wang, Y., Tian, Y., Guo, Y., & Wang, H. (2024). Active torque-based gait adjustment multi-level control strategy for lower limb patient-exoskeleton coupling system in rehabilitation training. *Mathematics and Computers in Simulation*, 215, 357–381.
- Wang, H.-H., Tsai, W.-C., Chang, C.-Y., Hung, M.-H., Tu, J.-H., Wu, T., et al. (2023). Effect of load carriage lifestyle on kinematics and kinetics of gait. *Applied Bionics and Biomechanics*, 2023.
- Wang, Y., & Wang, H. (2020). Gait learning for lower limb rehabilitation exoskeleton using dynamical movement primitives based on general regression neural networks. In *2020 Chinese automation congress* (pp. 7046–7051). IEEE.
- Wang, T., Zhao, J., Sui, D., Zhao, S., & Zhu, Y. (2022). A rhythmic motion control method inspired by board shoe racing for a weight-bearing exoskeleton. *Journal of Bionic Engineering*, 19(2), 403–415.
- Wu, Q., Liu, C., Zhang, J., & Chen, Q. (2009). Survey of locomotion control of legged robots inspired by biological concept. *Science in China Series F: Information Sciences*, 52(10), 1715–1729.
- Xu, D., Huang, P., Li, Z., & Feng, Y. (2022). Dmp-based motion generation for a walking exoskeleton robot using divergent component of motion. In *2022 international conference on advanced robotics and mechatronics* (pp. 232–237). IEEE.
- Xu, F., Qiu, J., Yuan, W., & Cheng, H. (2021). A novel balance control strategy based on enhanced stability pyramid index and dynamic movement primitives for a lower limb human-exoskeleton system. *Frontiers in Neurorobotics*, 15, Article 751642.
- Yingxu, W., Aibin, Z., Hongling, W., Pengcheng, Z., Zhang, X., & Guangzhong, C. (2019). Control of lower limb rehabilitation exoskeleton robot based on cpg neural network. In *2019 16th international conference on ubiquitous robots* (pp. 678–682). IEEE.
- Young, A. J., & Ferris, D. P. (2016). State of the art and future directions for lower limb robotic exoskeletons. *IEEE Transactions on Neural Systems and Rehabilitation Engineering*, 25(2), 171–182.
- Yu, J., Tan, M., Chen, J., & Zhang, J. (2013). A survey on cpg-inspired control models and system implementation. *IEEE Transactions on Neural Networks and Learning Systems*, 25(3), 441–456.
- Yuan, Y., Li, Z., Zhao, T., & Gan, D. (2019). Dmp-based motion generation for a walking exoskeleton robot using reinforcement learning. *IEEE Transactions on Industrial Electronics*, 67(5), 3830–3839.
- Zhang, X., Ge, W., Fu, H., Chen, R., Luo, T., & Hashimoto, M. (2018). A human–robot interaction based coordination control method for assistive walking devices and an assessment of its stability. *Mathematical Problems in Engineering*, 2018.
- Zhang, D., Ren, Y., Gui, K., Jia, J., & Xu, W. (2017). Cooperative control for a hybrid rehabilitation system combining functional electrical stimulation and robotic exoskeleton. *Frontiers in Neuroscience*, 11, 725.
- Zhang, P., & Zhang, J. (2022). Motion generation for walking exoskeleton robot using multiple dynamic movement primitives sequences combined with reinforcement learning. *Robotica*, 40(8), 2732–2747.
- Zou, C., Huang, R., Qiu, J., Chen, Q., & Cheng, H. (2020). Slope gradient adaptive gait planning for walking assistance lower limb exoskeletons. *IEEE Transactions on Automation Science and Engineering*, 18(2), 405–413.